Supplementary Materials: Reduction of 2,2′-Bipyridine by Quasi-Linear 3d-Metal(I) Silylamides—A Structural and Spectroscopic Study

Igor Müller, Christian Schneider, Clemens Pietzonka, Florian Kraus and C. Gunnar Werncke

Table of Contents

1. NMR Spectra

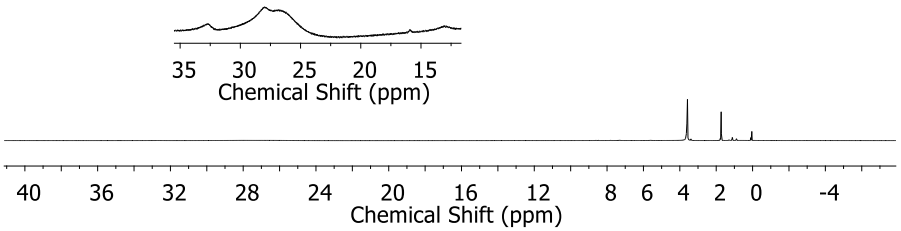

Figure S1. ^{1}H NMR spectrum of [K{18c6}][Cr(N(SiMe$_3$)$_2$)$_2$(bipy)] (**1**) in THF-d$_8$ (500.1 MHz).

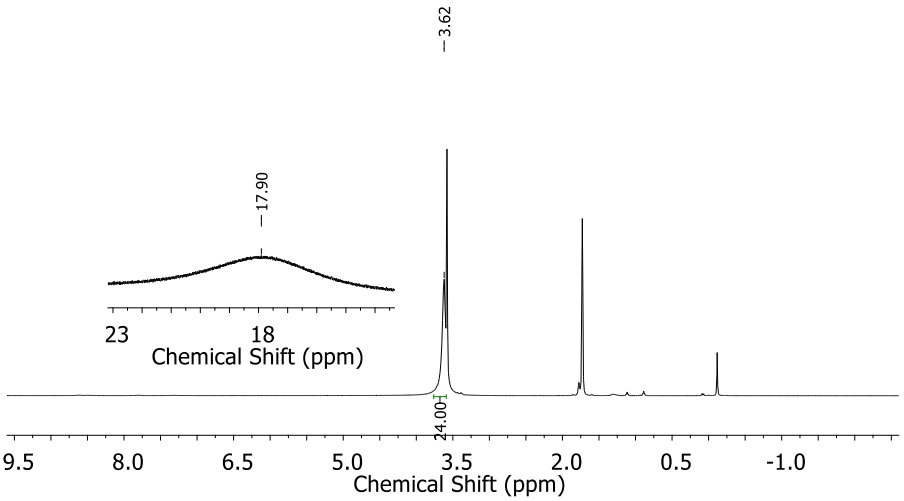

Figure S2. ^{1}H NMR spectrum of [K{18c6}][Mn(N(SiMe$_3$)$_2$)$_2$(bipy)] (**2**) in THF-d$_8$ (500.1 MHz).

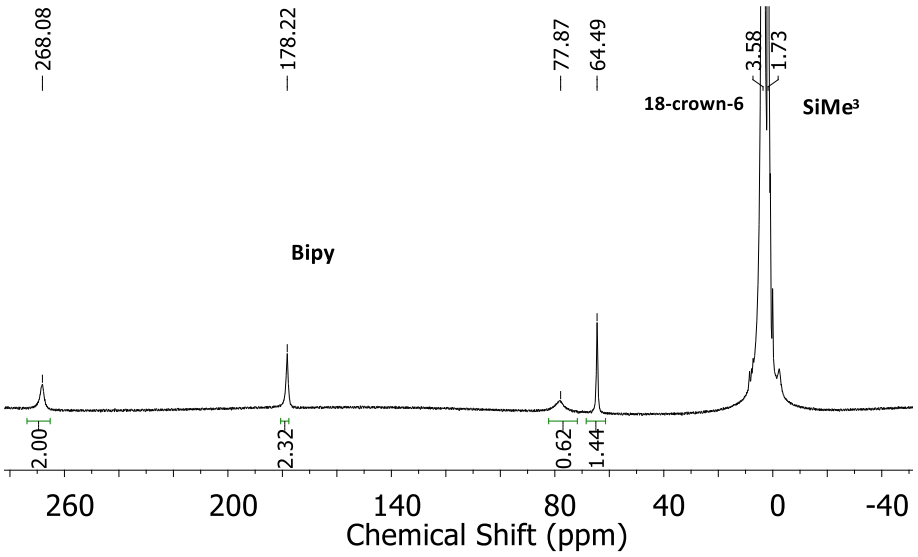

Figure S3. ^{1}H NMR spectrum of [K{18c6}][Fe(N(SiMe$_3$)$_2$)$_2$(bipy)] (**3**) in THF-d$_8$ (500.1 MHz).

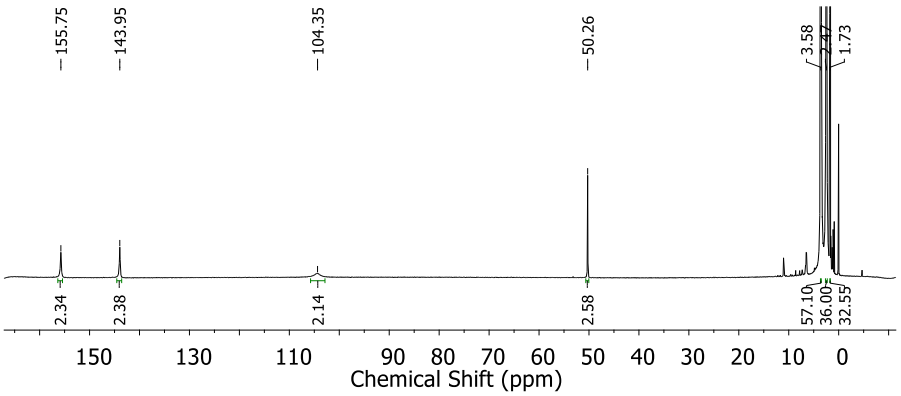

Figure S4. ^{1}H NMR spectrum of [K{18c6}][Co(N(SiMe$_3$)$_2$)$_2$(bipy)] (**4**) in THF-d$_8$ (500.1 MHz).

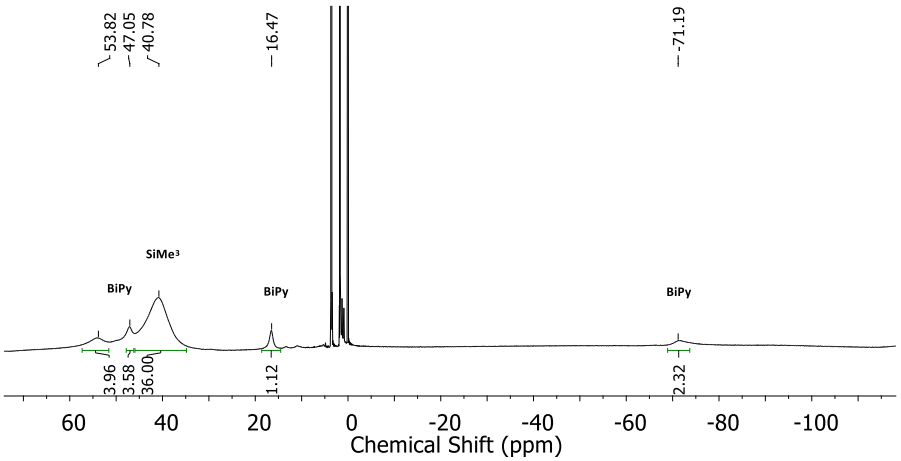

Figure S5. ^{1}H NMR spectrum of [Cr(N(SiMe$_3$)$_2$)$_2$(bipy)] (**5**) in THF-d$_8$ (500.1 MHz).

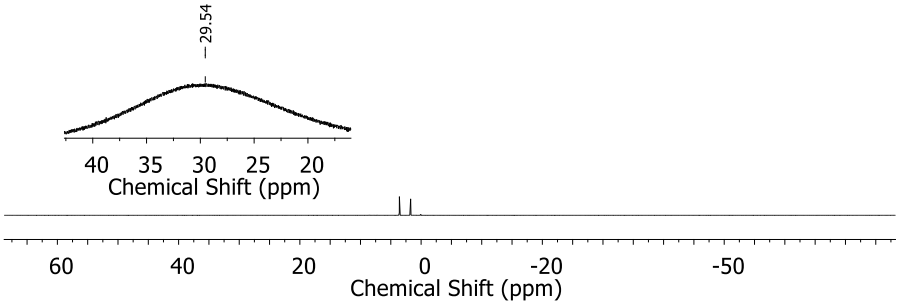

Figure S6. ^{1}H NMR spectrum of [Mn(N(SiMe$_3$)$_2$)$_2$(bipy)] (**6**) in THF-d$_8$ (500.1 MHz).

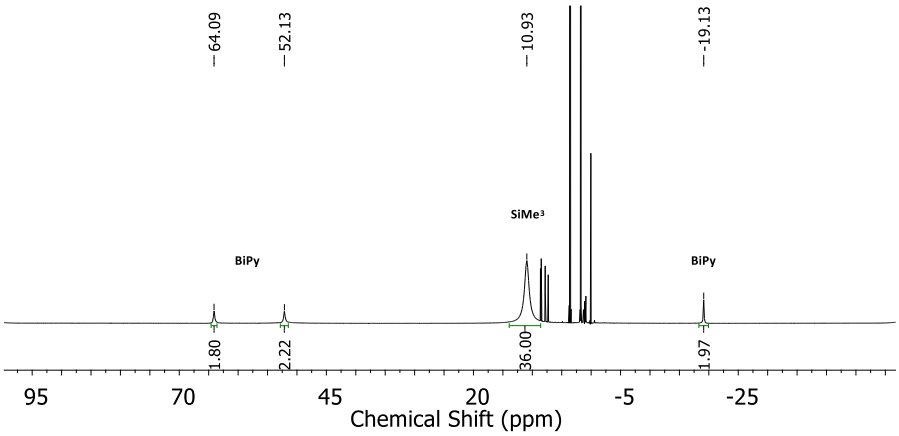

Figure S7. ^{1}H NMR spectrum of [Fe(N(SiMe$_3$)$_2$)$_2$(bipy)] (**7**) in THF-d$_8$ (500.1 MHz).

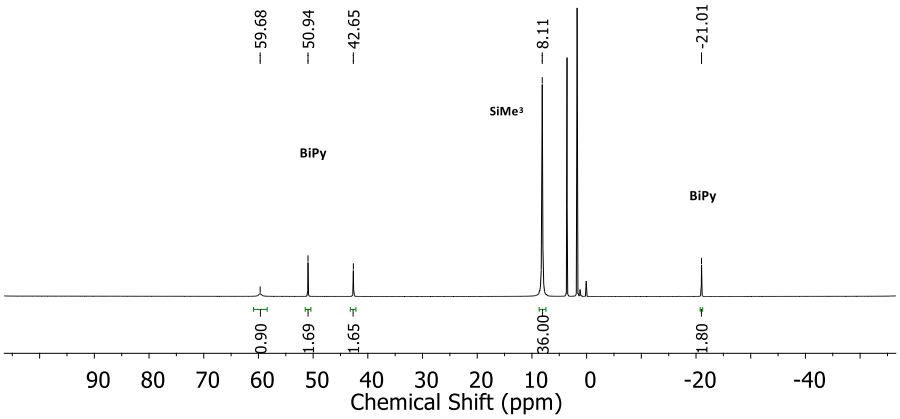

Figure S8. ^{1}H NMR spectrum of [Co(N(SiMe$_3$)$_2$)$_2$(bipy)] (**8**) in THF-d$_8$ (500.1 MHz).

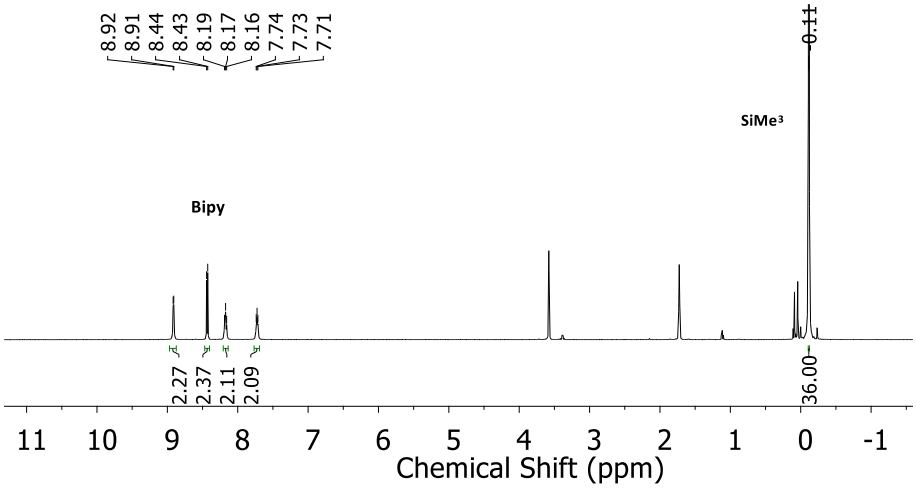

Figure S9. ^{1}H NMR spectrum of [Zn(N(SiMe$_3$)$_2$)$_2$(bipy)] (**9**) in THF-d$_8$ (500.1 MHz).

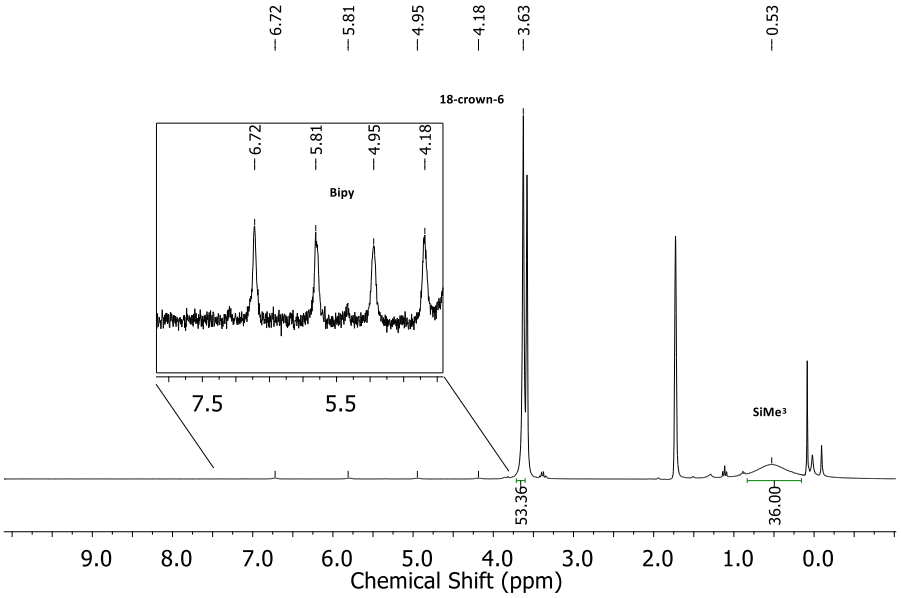

Figure S10. ^{1}H NMR spectrum of [K{18c6}][Zn(N(SiMe$_3$)$_2$)$_2$(BiPy)] (**10**) in THF-d$_8$ (500.1 MHz).

2. IR Spectra

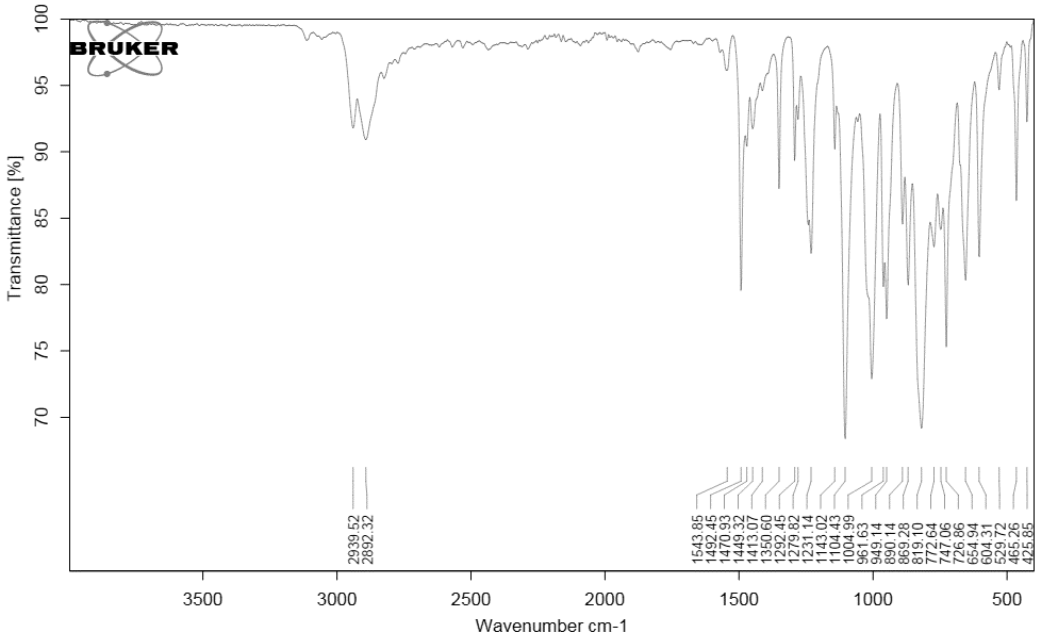

Figure S11. IR spectrum of [K{18c6}][Cr(N(SiMe$_3$)$_2$)$_2$(bipy)] (**1**).

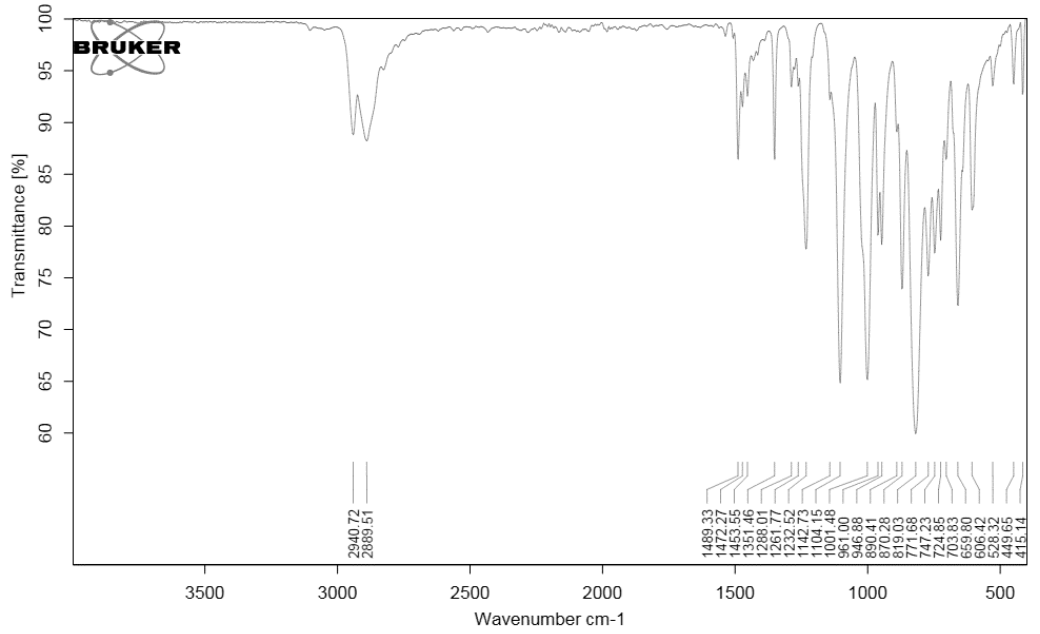

Figure S12. IR spectrum of [K{18c6}][Mn(N(SiMe$_3$)$_2$)$_2$(bipy)] (**2**).

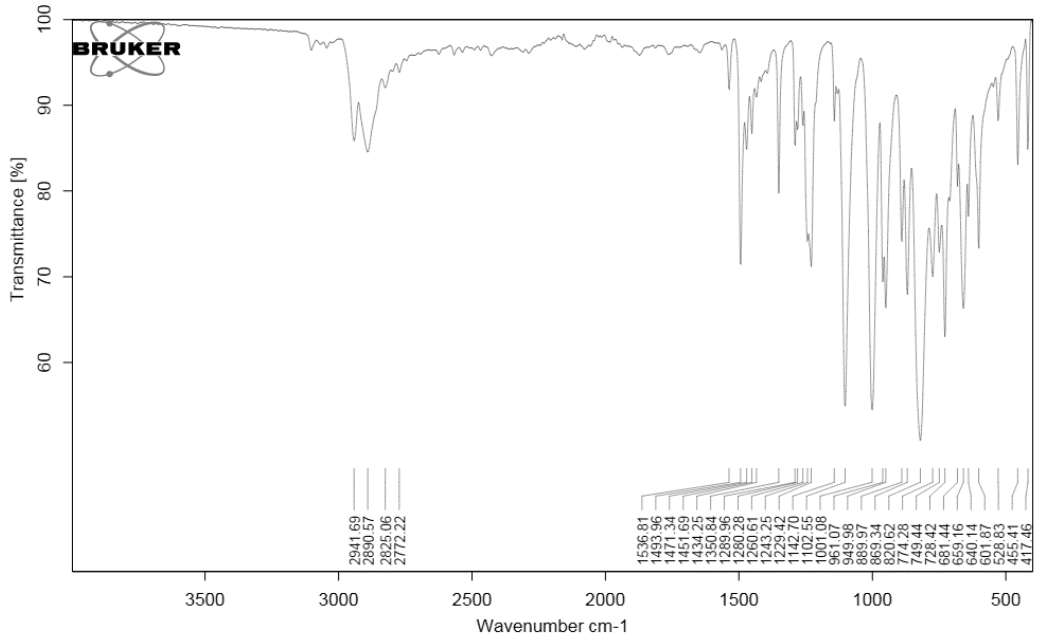

Figure S13. IR spectrum of [K{18c6}][Fe(N(SiMe$_3$)$_2$)$_2$(bipy)] (**3**).

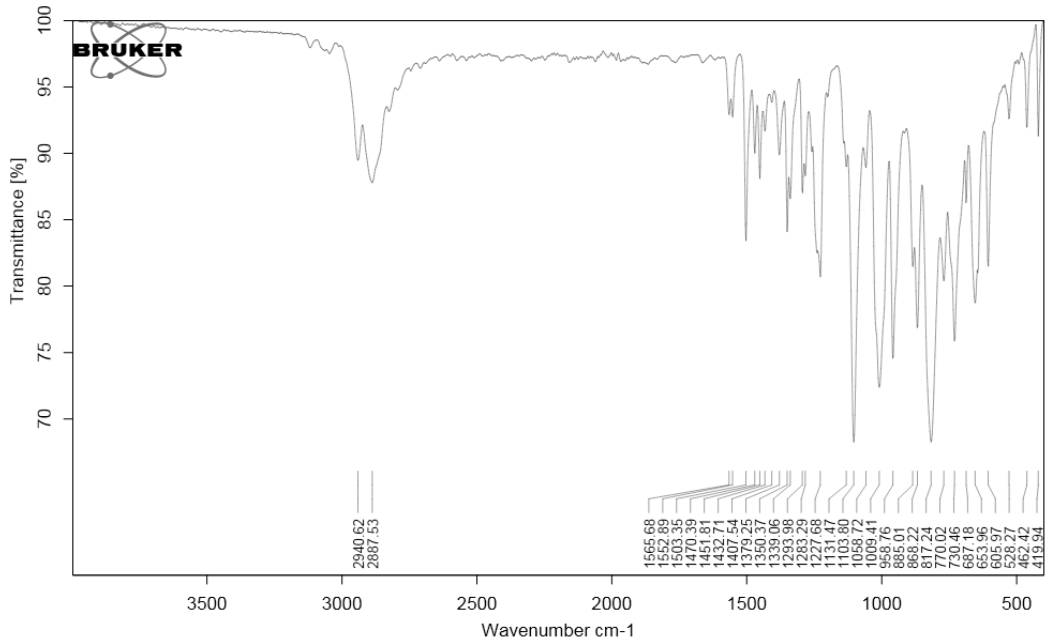

Figure S14. IR spectrum of [K{18c6}][Co(N(SiMe$_3$)$_2$)$_2$(bipy)] (**4**).

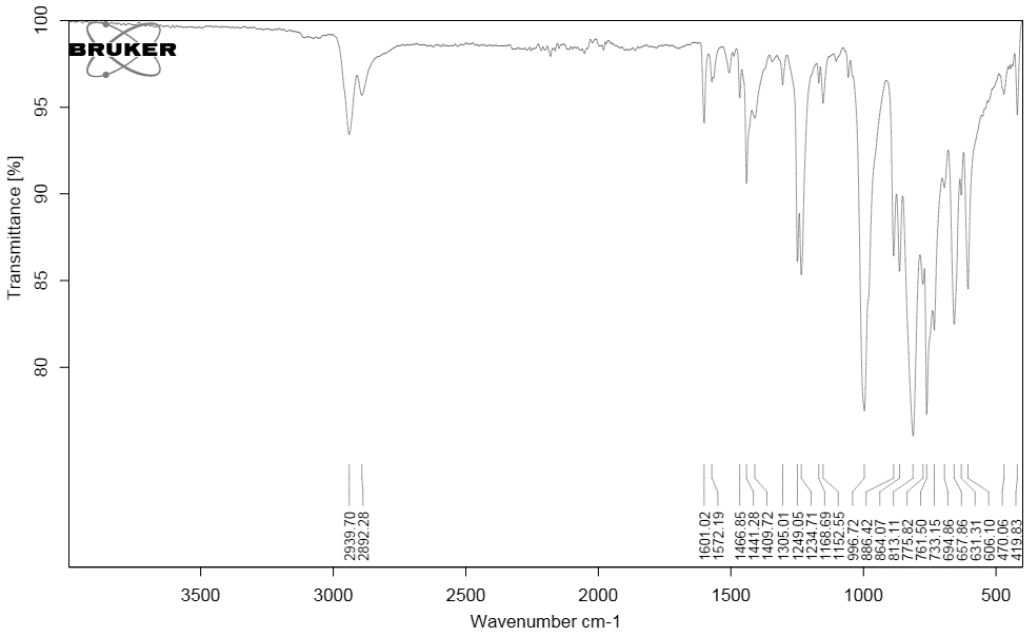

Figure S15. IR spectrum of [Cr(N(SiMe$_3$)$_2$)$_2$(bipy)] (**5**).

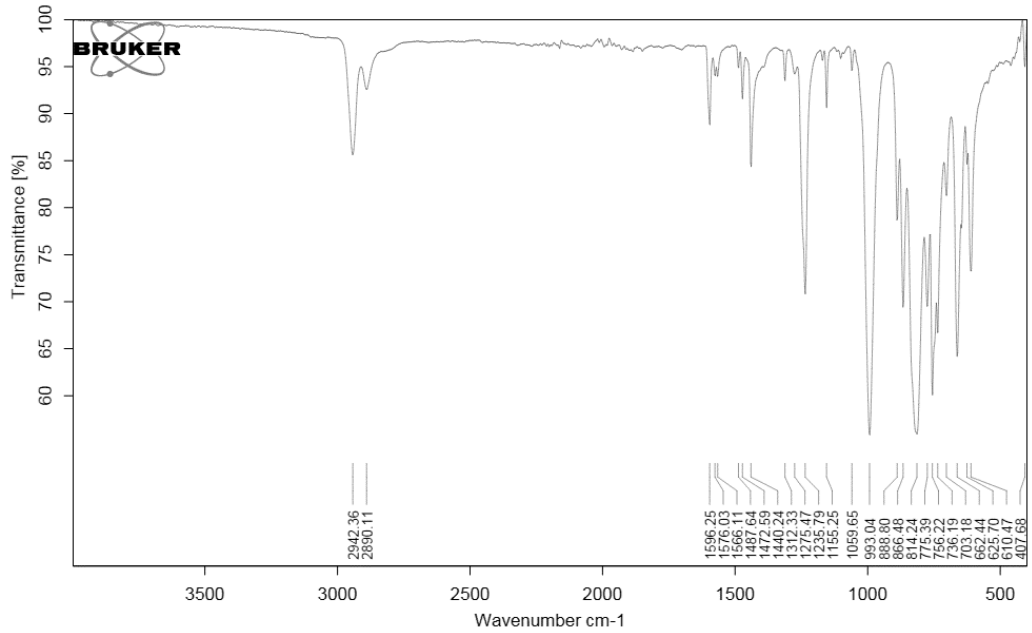

Figure S16. IR spectrum of [Mn(N(SiMe$_3$)$_2$)$_2$(bipy)] (**6**).

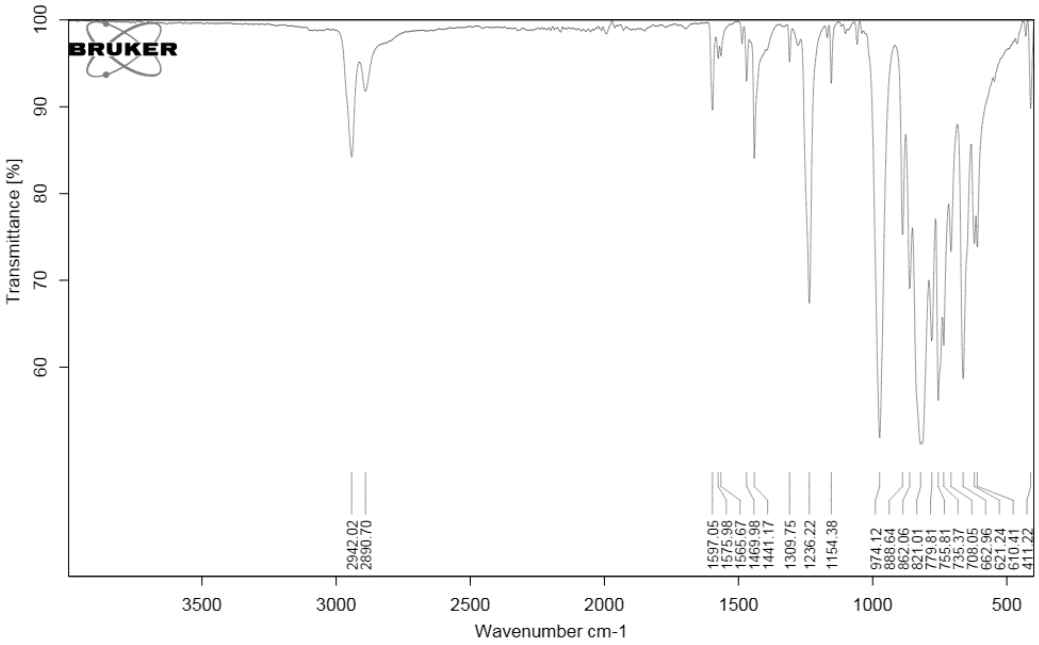

Figure S17. IR spectrum of [Fe(N(SiMe$_3$)$_2$)$_2$(bipy)] (**7**).

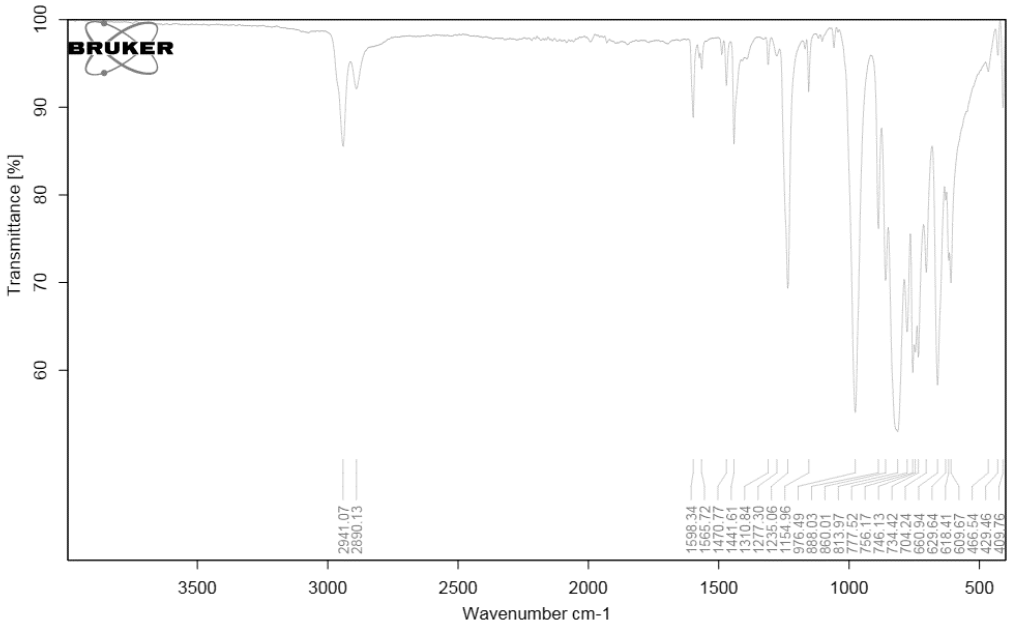

Figure S18. IR spectrum of [Co(N(SiMe$_3$)$_2$)$_2$(bipy)] (**8**).

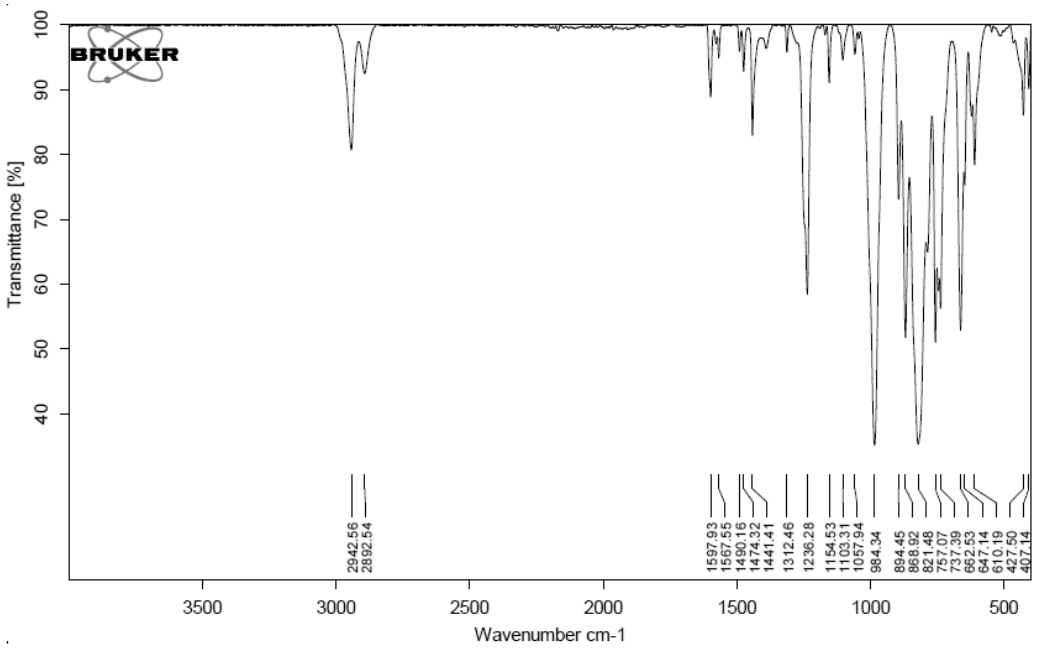

Figure S19. IR spectrum of [Zn(N(SiMe$_3$)$_2$)$_2$(bipy)] (**9**).

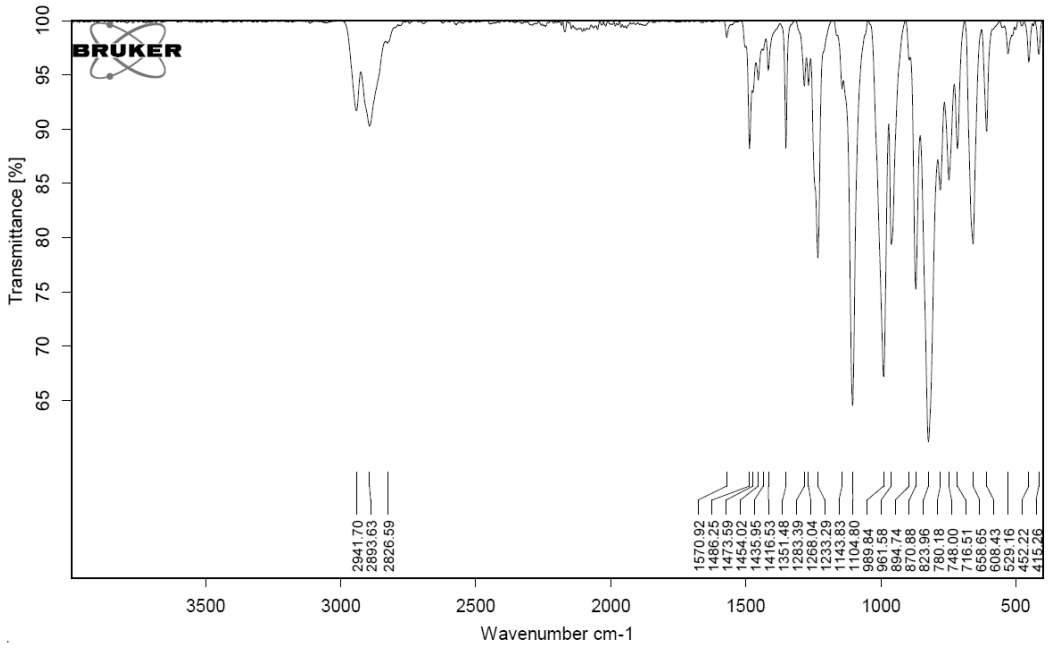

Figure S20. IR spectrum of [K{18c6}][Zn(N(SiMe$_3$)$_2$)$_2$(bipy)] (**10**).

3. UV/Vis Spectra

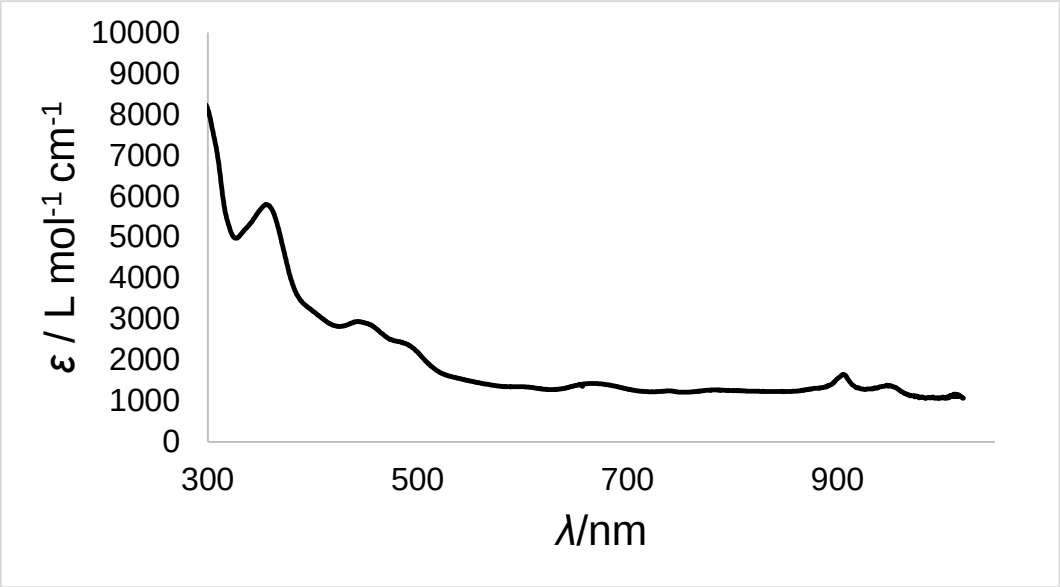

Figure S21. UV/Vis spectrum of [K{18c6}][Cr(N(SiMe$_3$)$_2$)$_2$(bipy)] (**1**) in Et$_2$O.

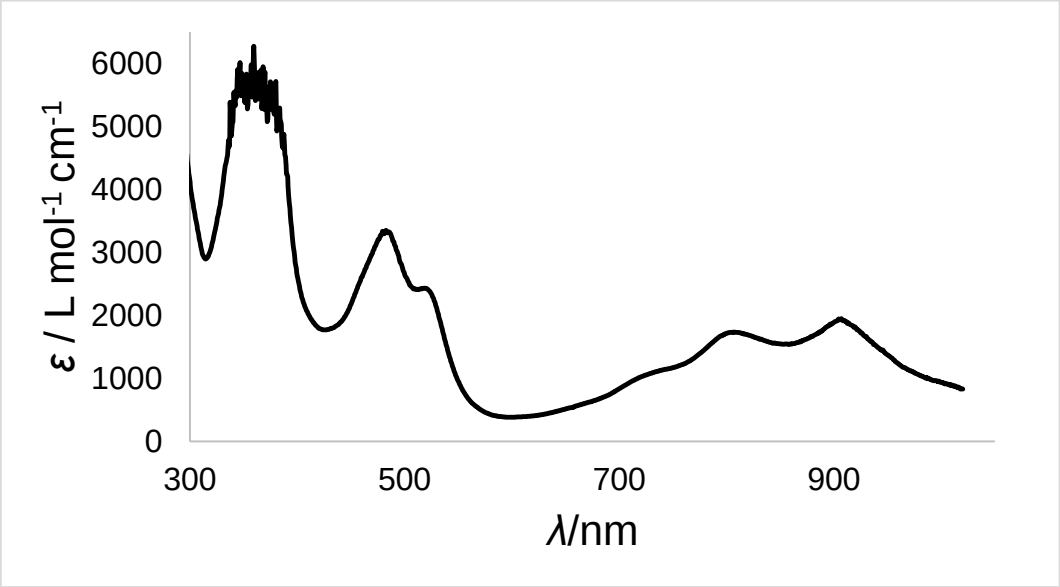

Figure S22. UV/Vis spectrum of [K{18c6}][Mn(N(SiMe$_3$)$_2$)$_2$(bipy)] (**2**) in Et$_2$O.

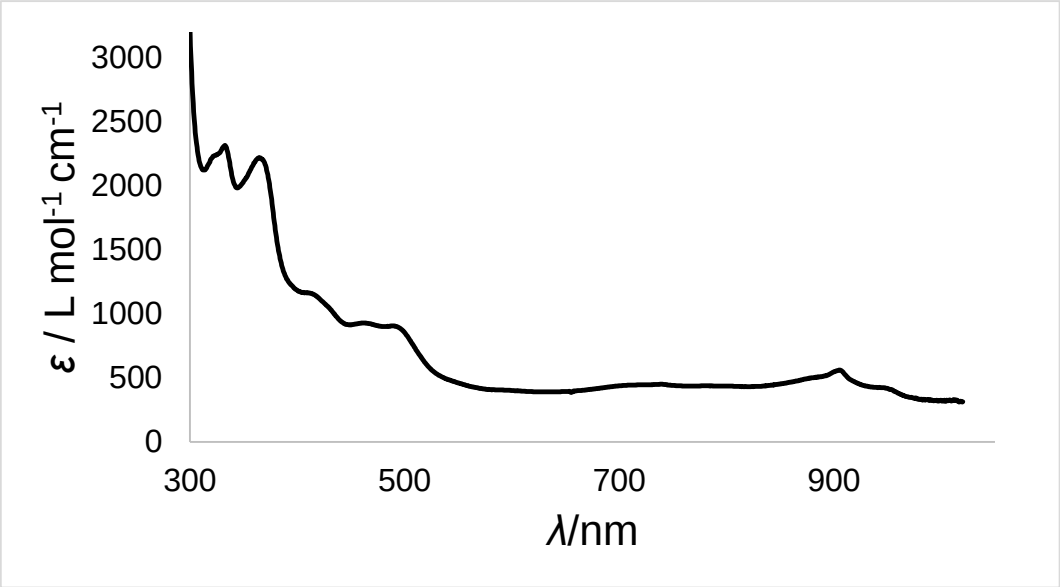

Figure S23. UV/Vis spectrum of [K{18c6}][Fe(N(SiMe$_3$)$_2$)$_2$(bipy)] (**3**) in Et$_2$O.

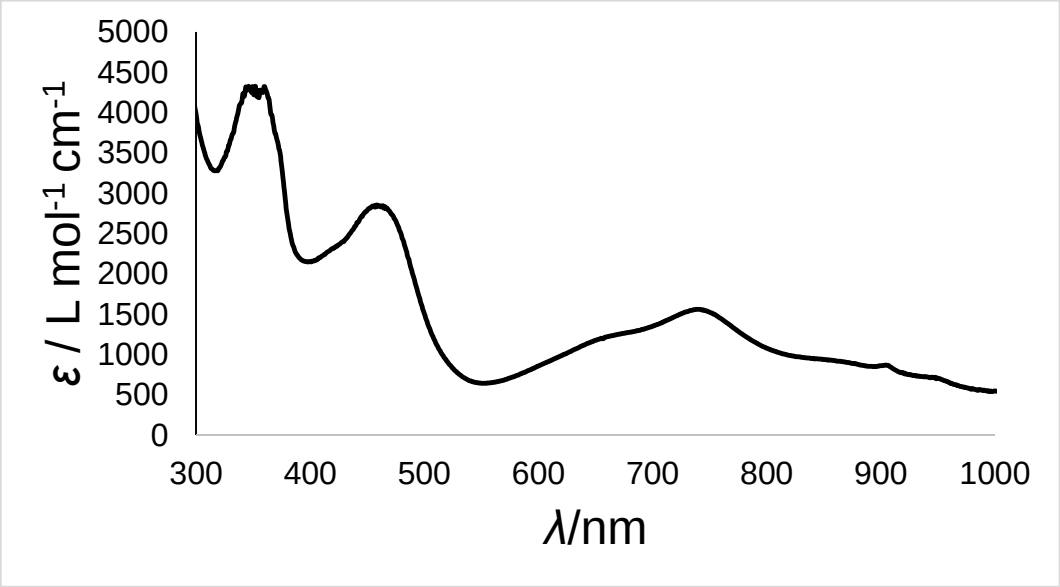

Figure S24. UV/Vis spectrum of [K{18c6}][Co(N(SiMe$_3$)$_2$)$_2$(bipy)] (**4**) in Et$_2$O.

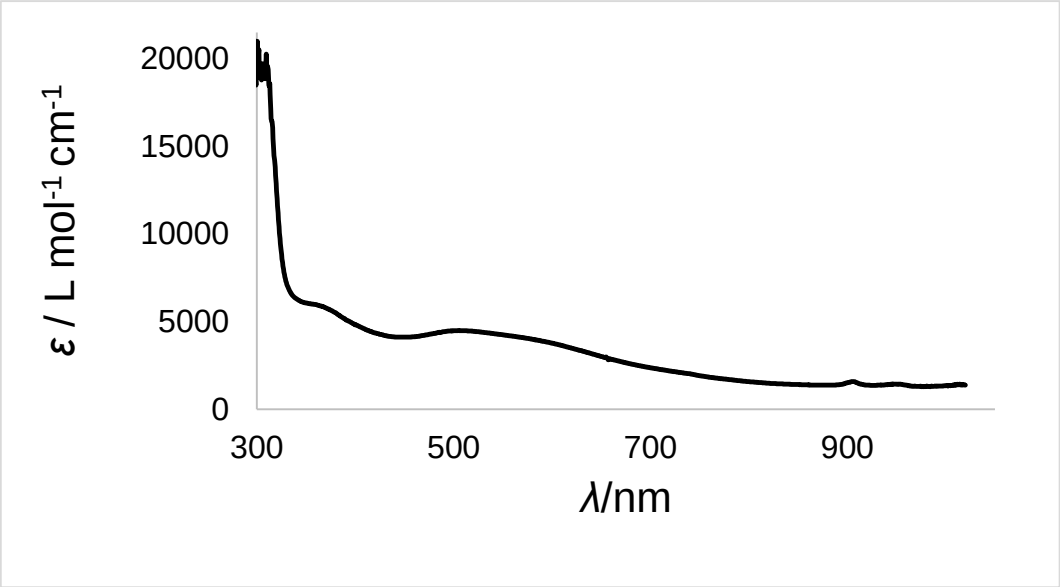

Figure S25. UV/Vis spectrum of [Cr(N(SiMe$_3$)$_2$)$_2$(bipy)] (**5**) in Et$_2$O.

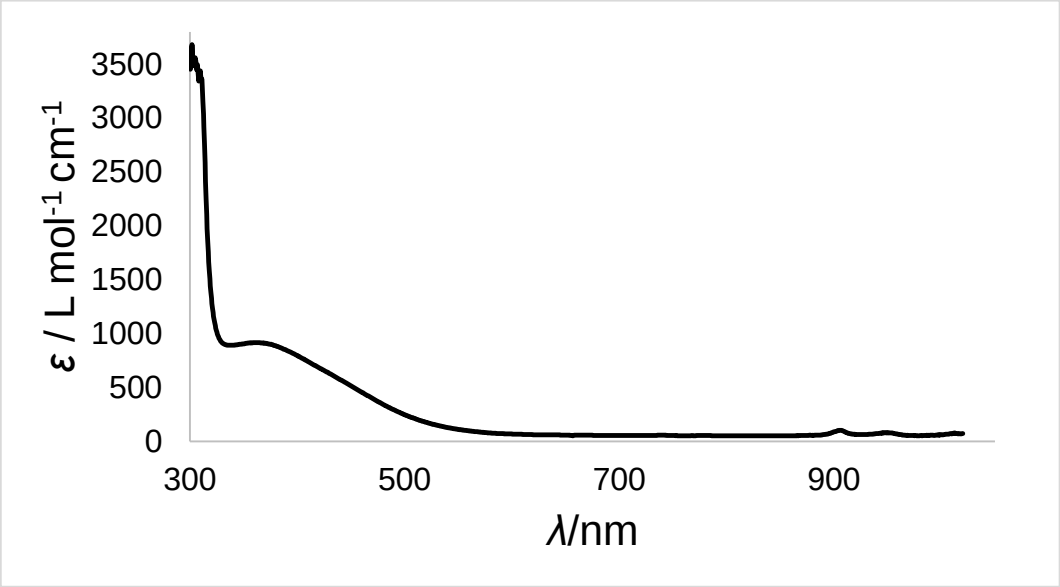

Figure S26. UV/Vis spectrum of [Mn(N(SiMe$_3$)$_2$)$_2$(bipy)] (**6**) in Et$_2$O.

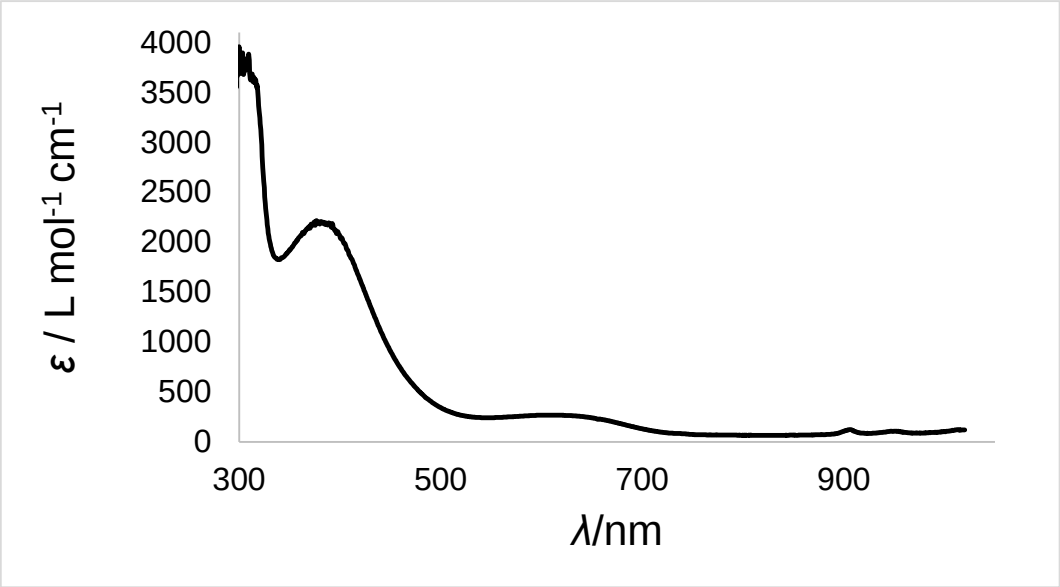

Figure S27. UV/Vis spectrum of [Fe(N(SiMe$_3$)$_2$)$_2$(bipy)] (**7**) in Et$_2$O.

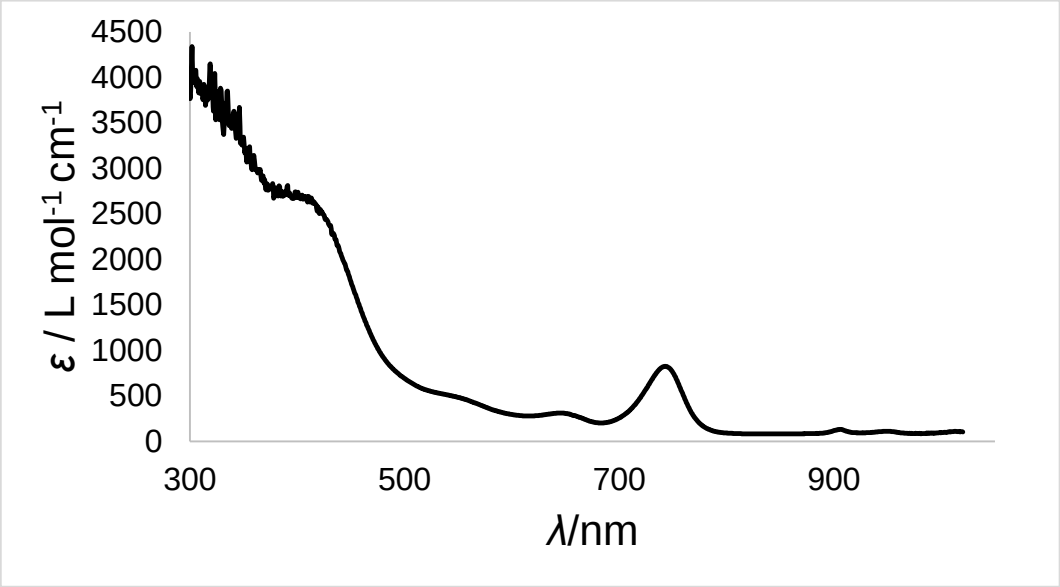

Figure S28. UV/Vis spectrum of [Co(N(SiMe$_3$)$_2$)$_2$(bipy)] (**8**) in Et$_2$O.

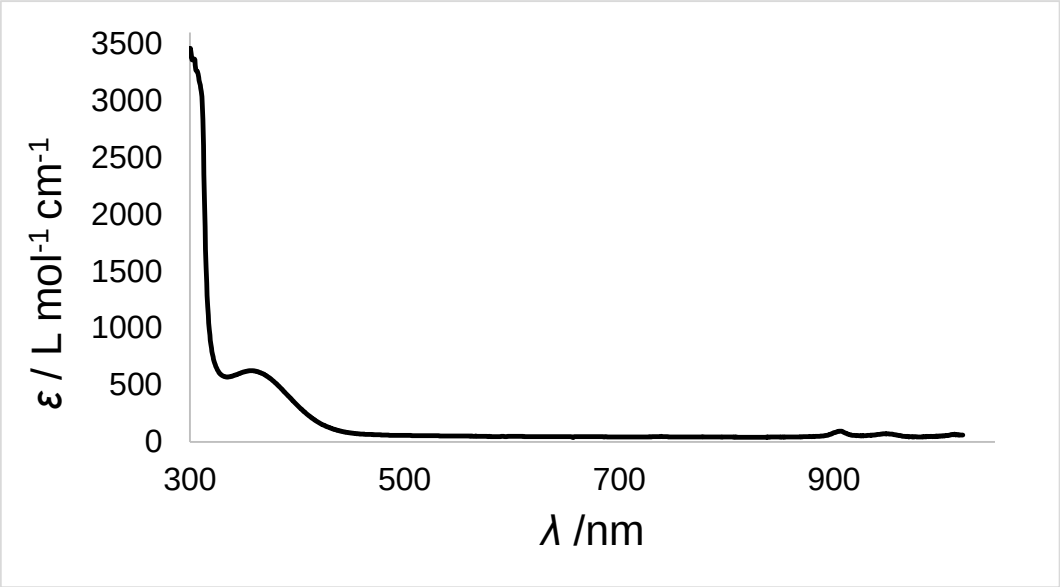

Figure S29. UV/Vis spectrum of [Zn(N(SiMe$_3$)$_2$)$_2$(bipy)] (**9**) in Et$_2$O.

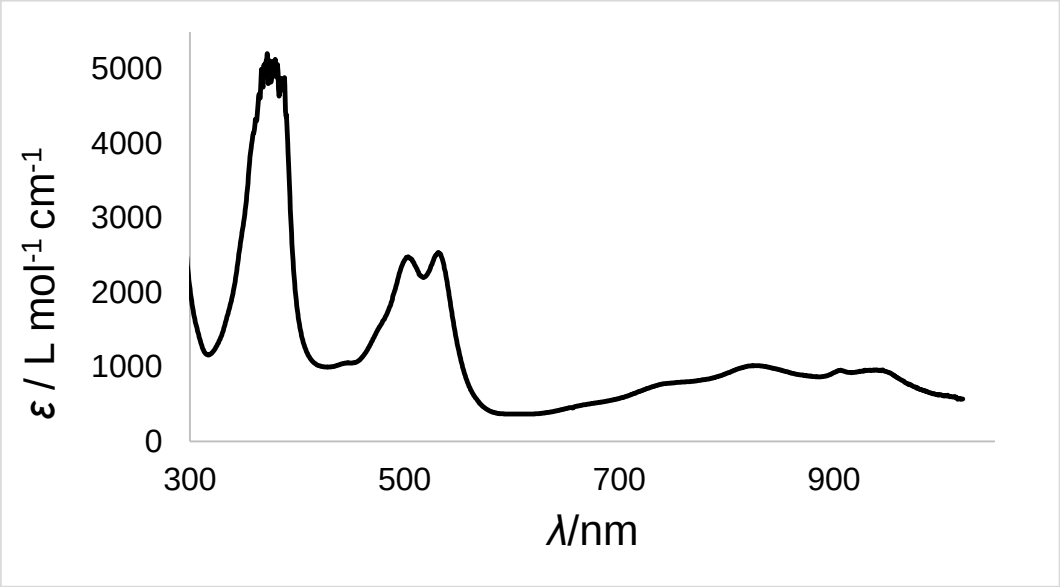

Figure S30. UV/Vis spectrum of [K{18c6}][Zn(N(SiMe$_3$)$_2$)$_2$(bipy)] (**10**) in Et$_2$O.

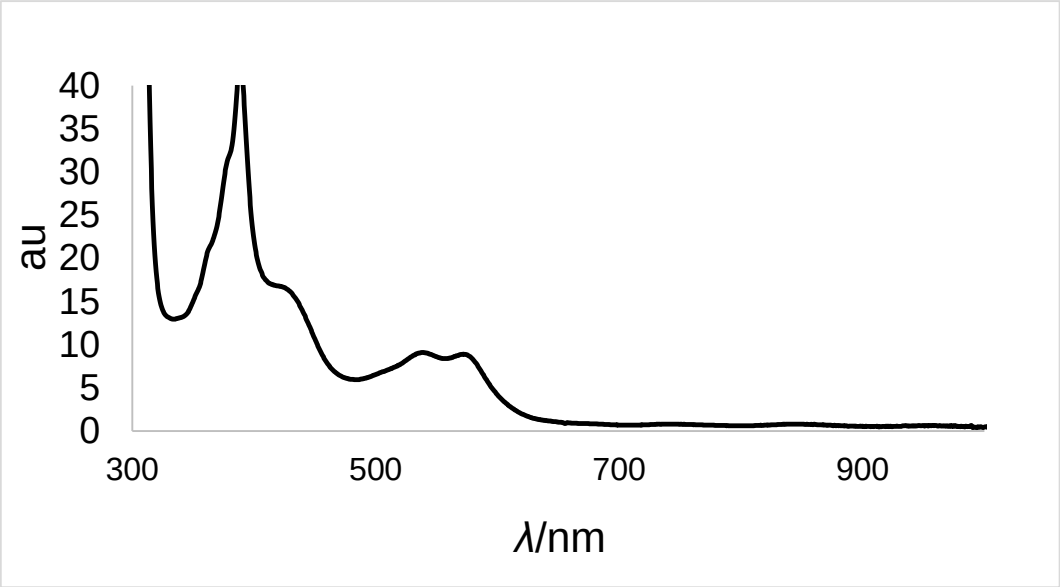

Figure S31. UV/Vis spectrum of [K{18c6}][(bipy)] in Et_2O. [K{18c6}][(bipy)] was obtained in-situ from a reaction of 2,2´-bipyridine with KC_8 in the presence of 18-crown-6 in Et_2O.

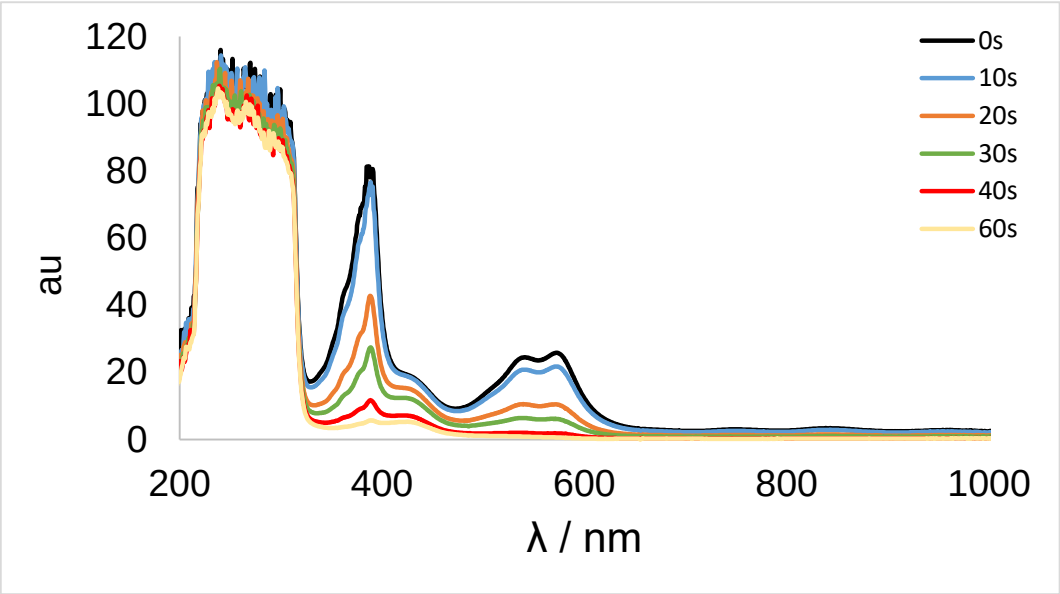

Figure S32. Time-dependent UV/Vis spectra of in-situ synthesized [K{18c6}][(bipy)] in Et_2O.

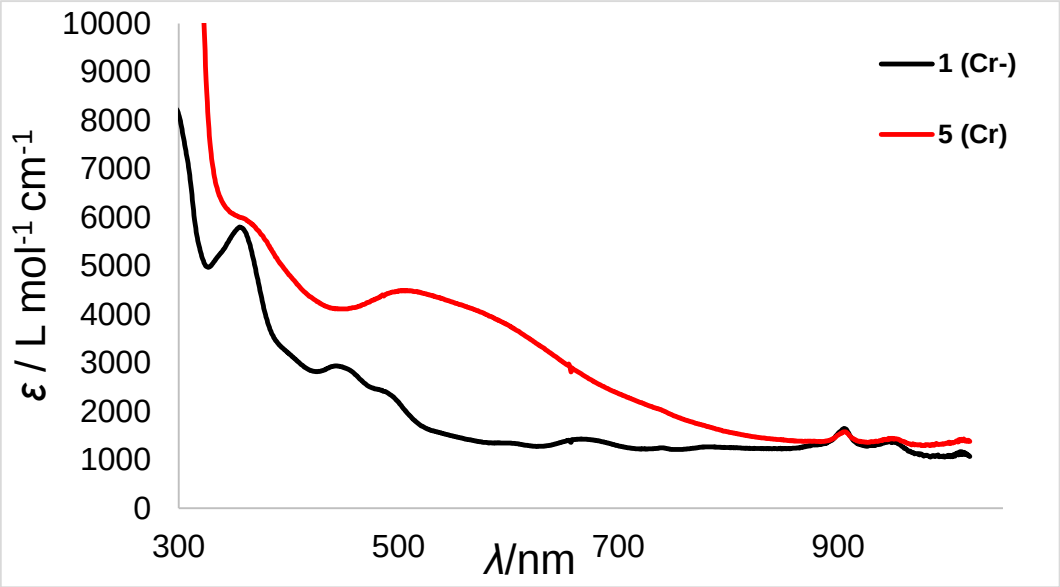

Figure S33. Overlay of UV/Vis spectra of [K{18c6}][Cr(N(SiMe$_3$)$_2$)$_2$(bipy)] (**1**) and [Cr(N(SiMe$_3$)$_2$)$_2$(bipy)] (**5**) in Et$_2$O.

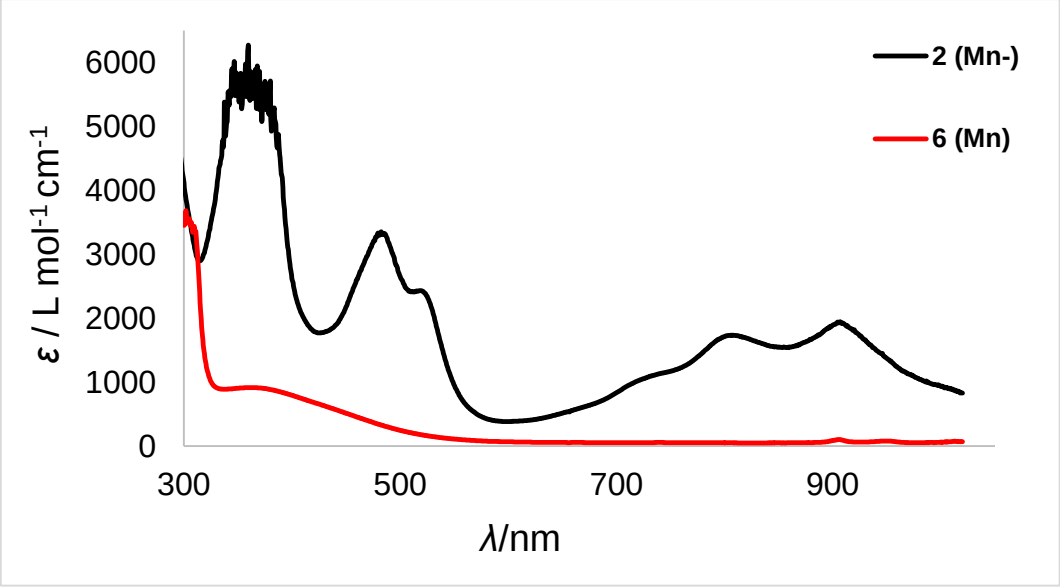

Figure S34. Overlay of UV/Vis spectra of [K{18c6}][Mn(N(SiMe$_3$)$_2$)$_2$(bipy)] (**2**) and [Mn(N(SiMe$_3$)$_2$)$_2$(bipy)] (6) in Et$_2$O.

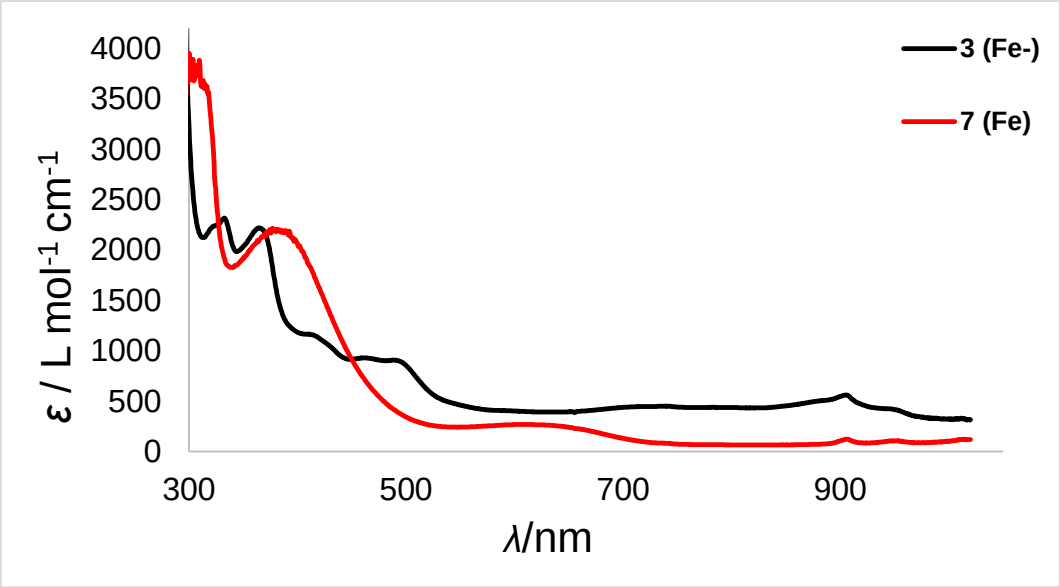

Figure S35. Overlay of UV/Vis spectra of [K{18c6}][Fe(N(SiMe$_3$)$_2$)$_2$(bipy)] (**3**) and [Fe(N(SiMe$_3$)$_2$)$_2$(bipy)](**7**) in Et$_2$O.

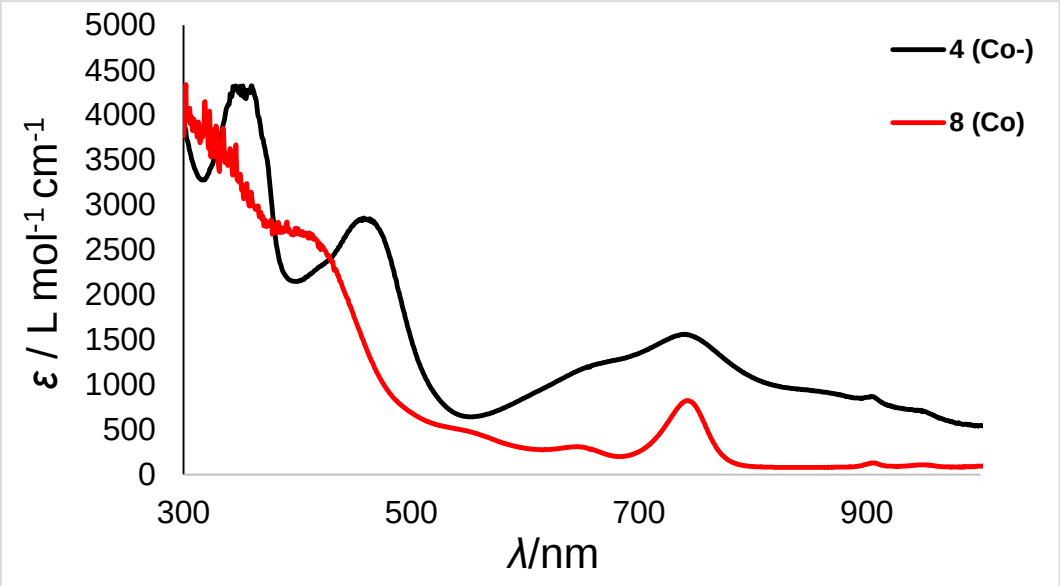

Figure S36. Overlay of UV/Vis spectra of [K{18c6}][Co(N(SiMe$_3$)$_2$)$_2$(bipy)] (**4**) [Co(N(SiMe$_3$)$_2$)$_2$(bipy)] (**8**) in Et$_2$O.

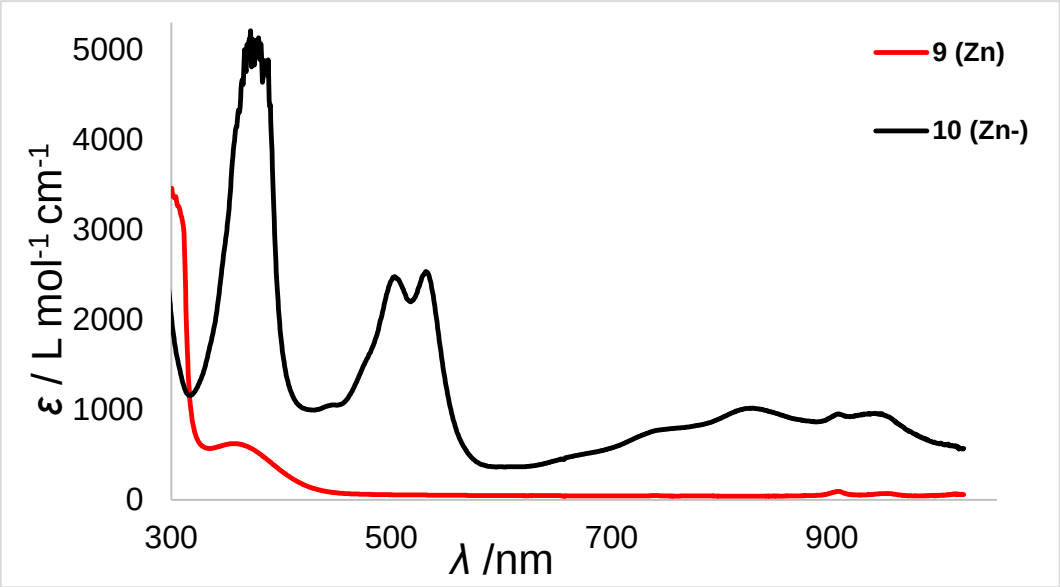

Figure S37. Overlay of UV/Vis spectra of [Zn(N(SiMe$_3$)$_2$)$_2$(bipy)] (**9**) and [K{18c6}][Zn(N(SiMe$_3$)$_2$)$_2$(bipy)] (**10**) in Et$_2$O.

4. Magnetic Data

Magnetic data of compounds **1**–**4** and **10** were recorded on dried crystalline samples and were corrected for diamagnetic contributions from the sample holder and the diamagnetic susceptibility of the respective compound using Pascal constants. Obtained paramagnetic susceptibility χ_{para} was fit using the Curie-Weiss-law $\chi_{CW} = (\frac{N_A \mu_B^2 n_{eff}}{3k_B})^2 \frac{1}{T-\theta}$ (n_{eff} = effective magnetic moment in Bohr's magnetons per formula unit, Θ = Weiss temperature) with contributions from a temperature independent paramagnetism χ_{TIP} using the overall equation $\chi_{para}T = (\chi_{TIP} + \chi_{CW})T$.

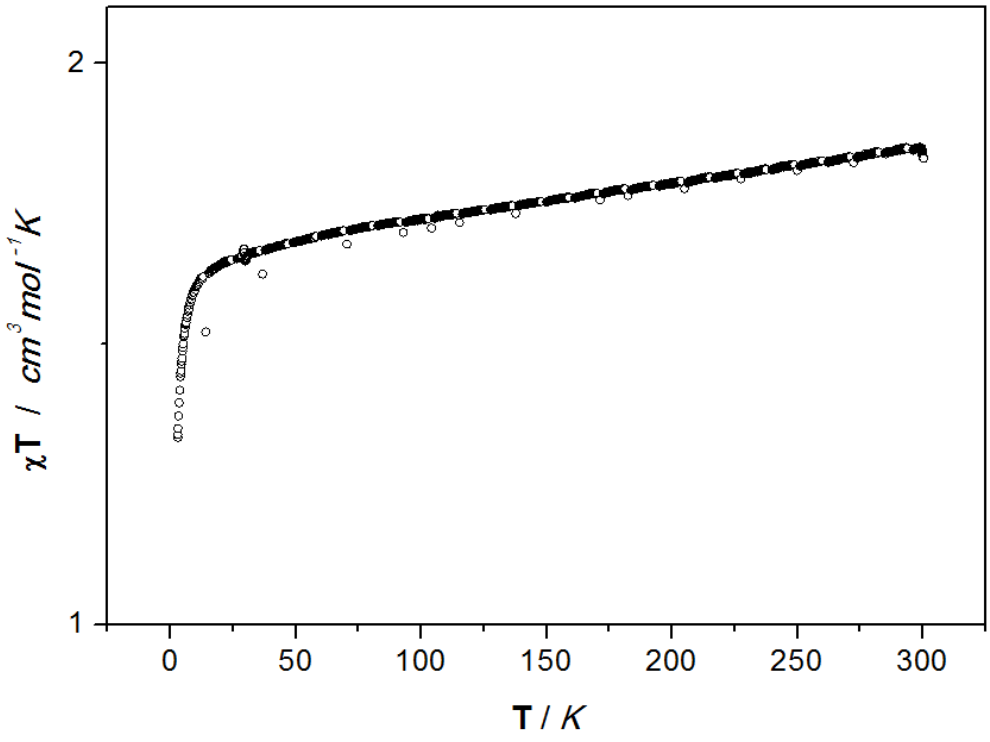

Figure S38. Temperature dependence of the molar magnetic susceptibility times temperature product (χT vs. T) for compound K{18c6}][Cr(N(SiMe$_3$)$_2$)$_2$(bipy)] (**1**). Data were collected under an applied dc field of 1 T in a temperature range of 3 to 300 K.

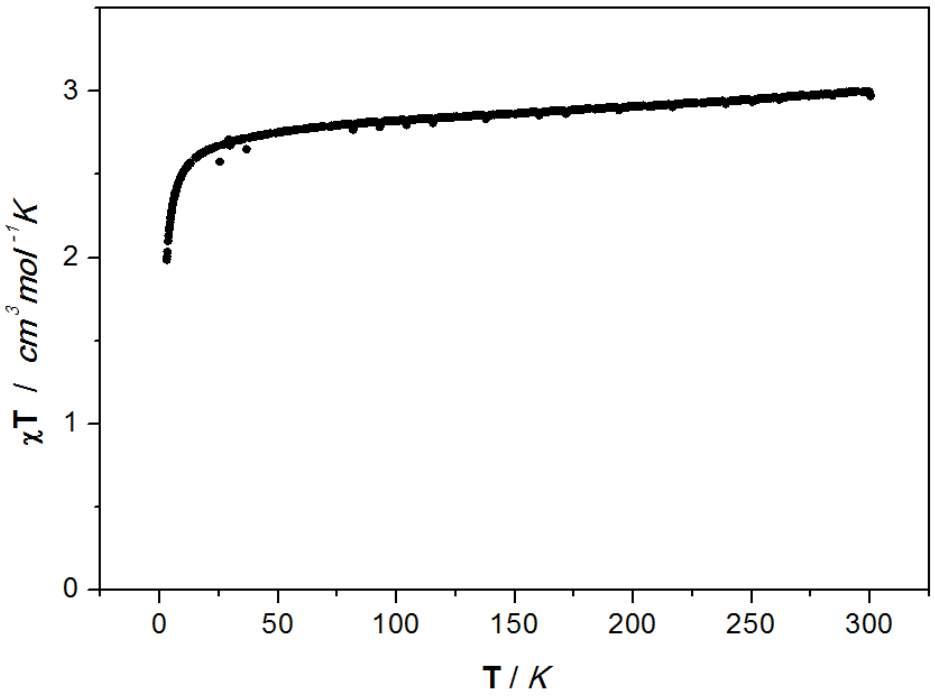

Figure S39. Temperature dependence of the molar magnetic susceptibility times temperature product (χT vs. T) for compound K{18c6}][Mn(N(SiMe$_3$)$_2$)$_2$(bipy)] (**2**). Data was collected under an applied dc field of 1 T in a temperature range of 3 to 300 K.

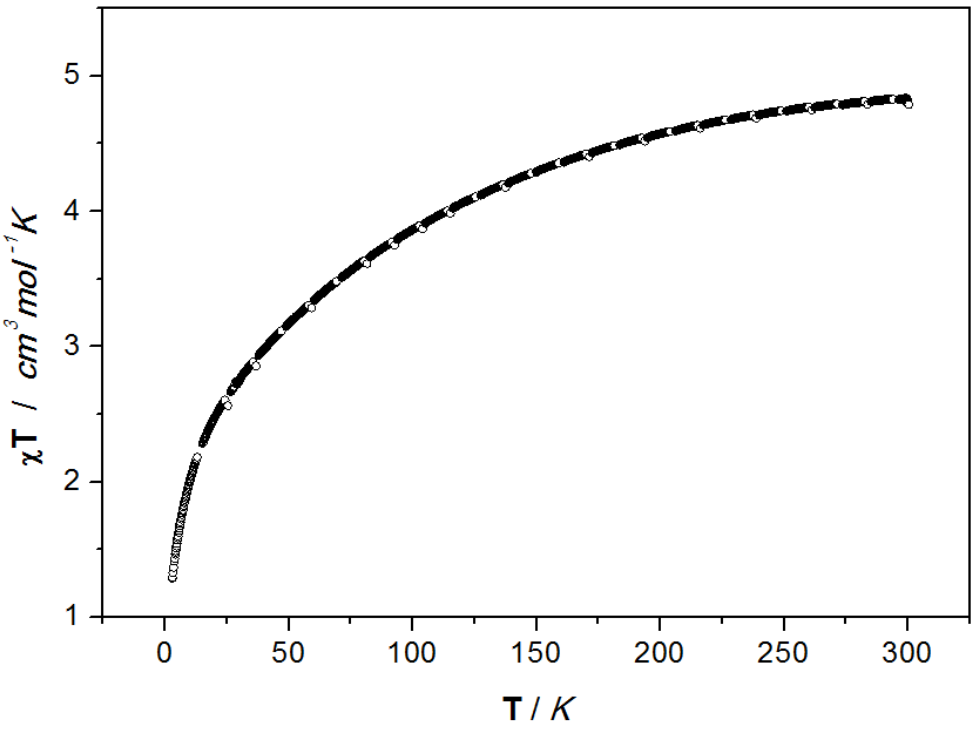

Figure S40. Temperature dependence of the molar magnetic susceptibility times temperature product (χT vs. T) for compound K{18c6}][Fe(N(SiMe$_3$)$_2$)$_2$(bipy)] (**3**). Data was collected under an applied dc field of 1 T in a temperature range of 3 to 300 K.

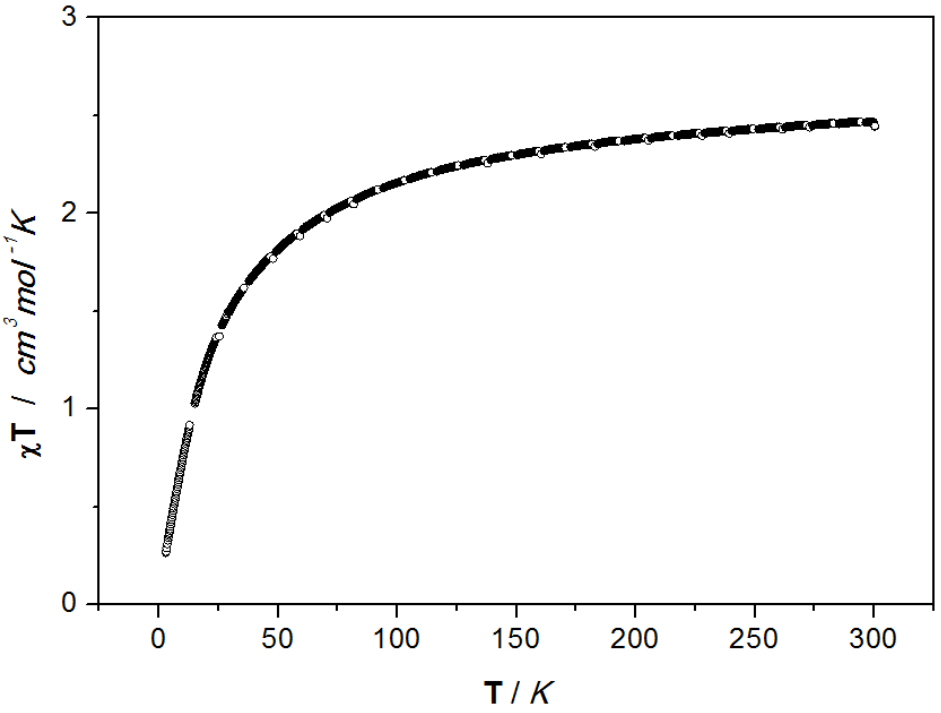

Figure S41. Temperature dependence of the molar magnetic susceptibility times temperature product (χT vs. T) for compound K{18c6}][Co(N(SiMe$_3$)$_2$)$_2$(bipy)] (**4**). Data was collected under an applied dc field of 1 T in a temperature range of 3 to 300 K.

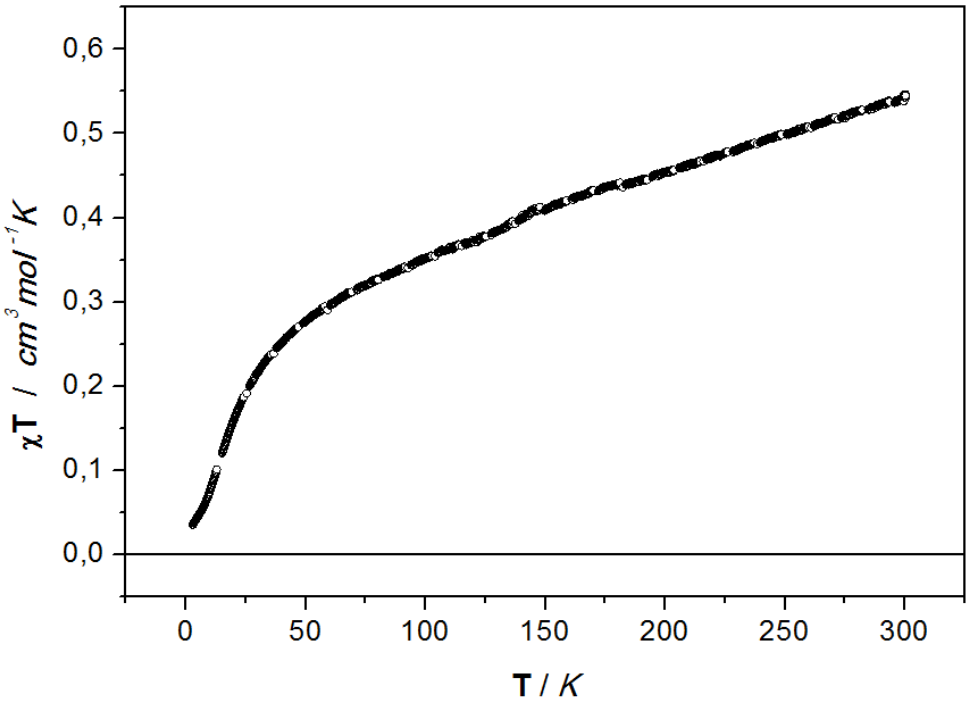

Figure S42. Temperature dependence of the molar magnetic susceptibility times temperature product (χT vs. T) for compound K{18c6}][Zn(N(SiMe$_3$)$_2$)$_2$(bipy)] (**10**). Data was collected under an applied dc field of 1 T in a temperature range of 3 to 300 K.

5. Cyclic Voltammetry

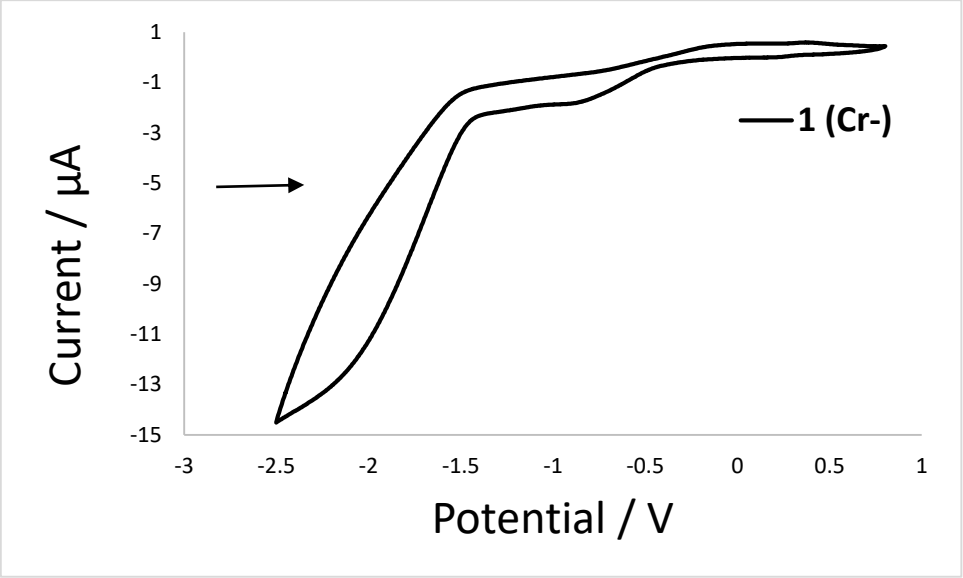

Figure S33. Cyclic voltammogram for complex **1** in THF (1 mM, 500 mV/s, 0.1 M [NBu$_4$][PF$_6$]).

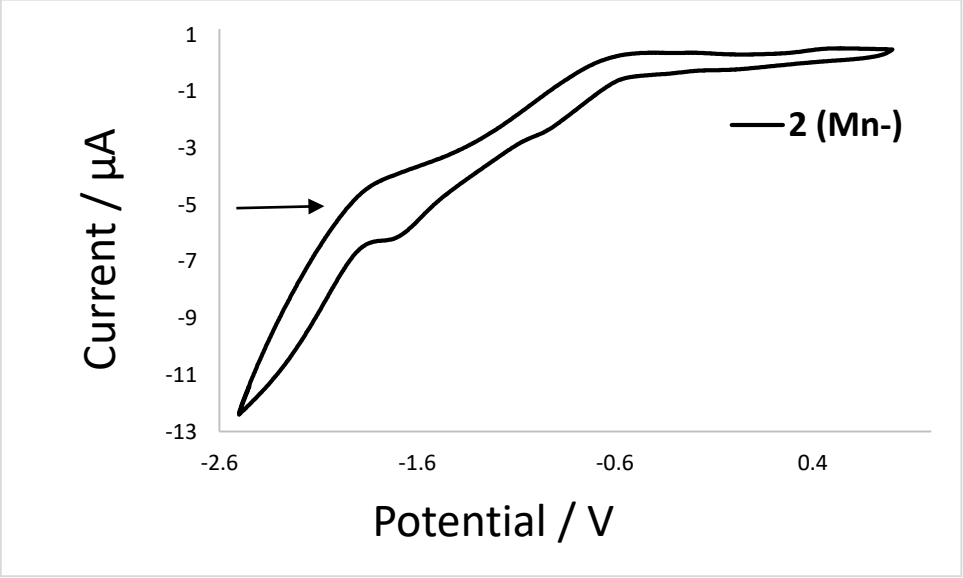

Figure S44. Cyclic voltammogram for complex **2** in THF (1 mM, 500 mV/s, 0.1 M [NBu$_4$][PF$_6$]).

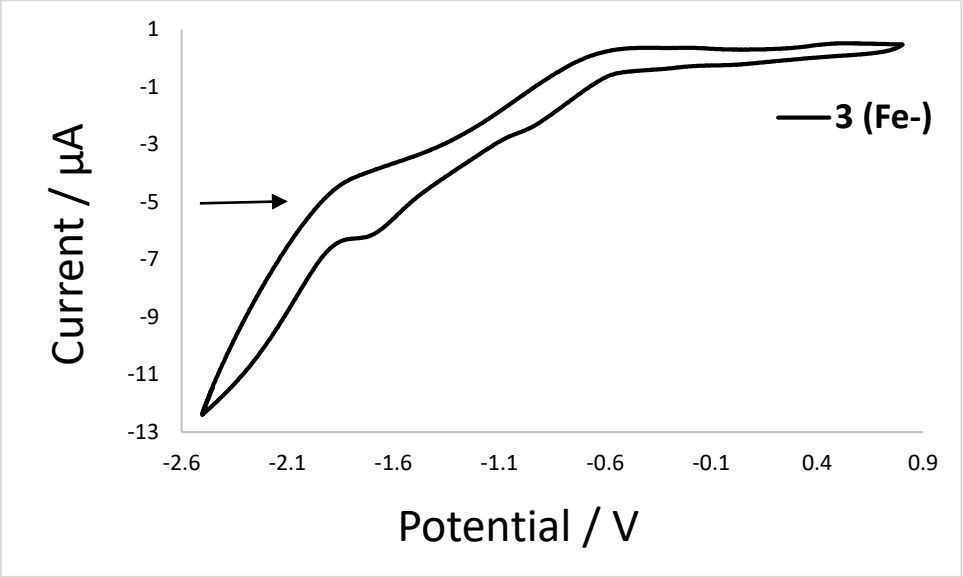

Figure S44. Cyclic voltammogram for complex **3** in THF (1 mM, 500 mV/s, 0.1 M [NBu$_4$][PF$_6$]).

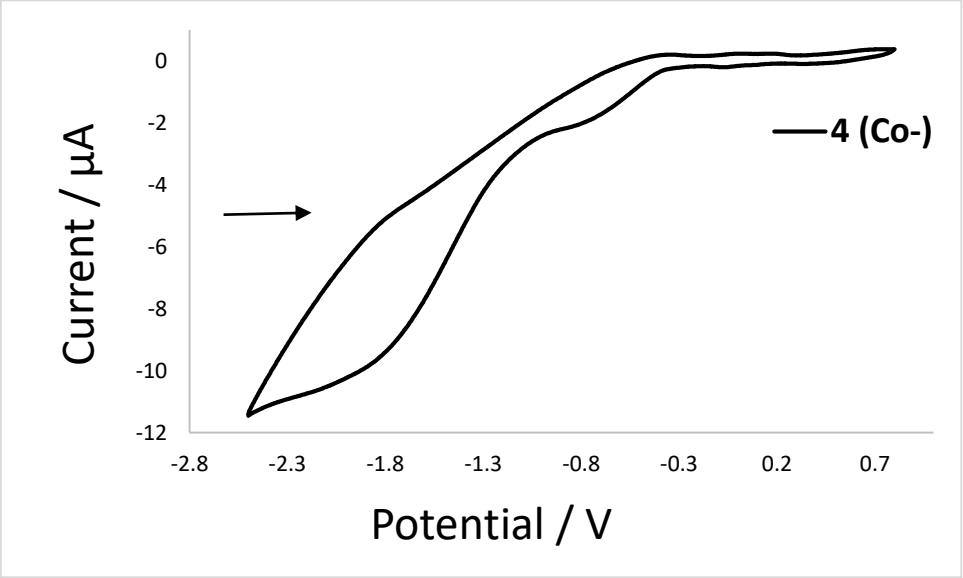

Figure S46. Cyclic voltammogram for complex **4** in THF (1 mM, 500 mV/s, 0.1 M [NBu$_4$][PF$_6$]).

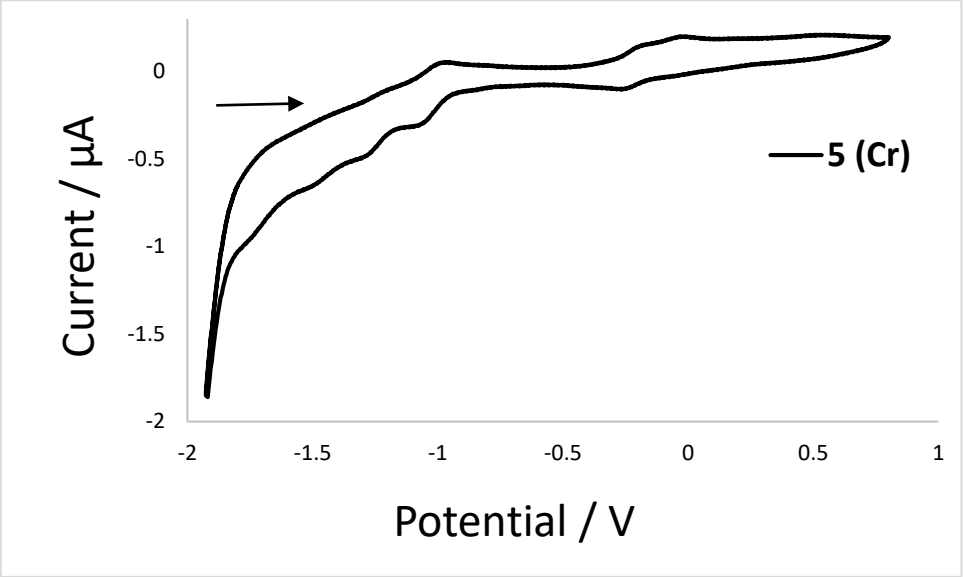

Figure S47. Cyclic voltammogram for complex **5** in THF (1 mM, 500 mV/s, 0.1 M [NBu$_4$][PF$_6$]).

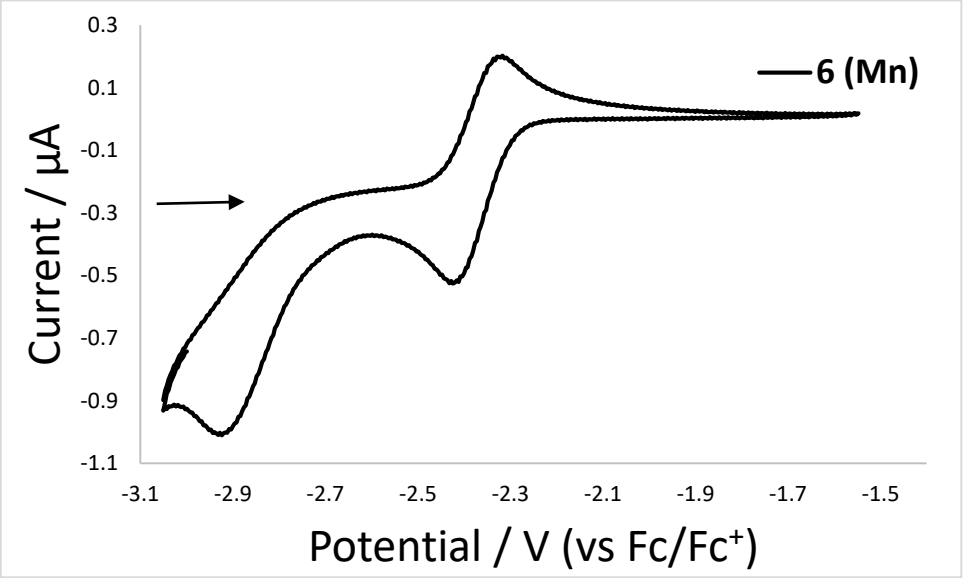

Figure S48. Cyclic voltammogram for complex **6** in THF (1 mM, 500 mV/s, 0.1 M [NBu$_4$][PF$_6$]).

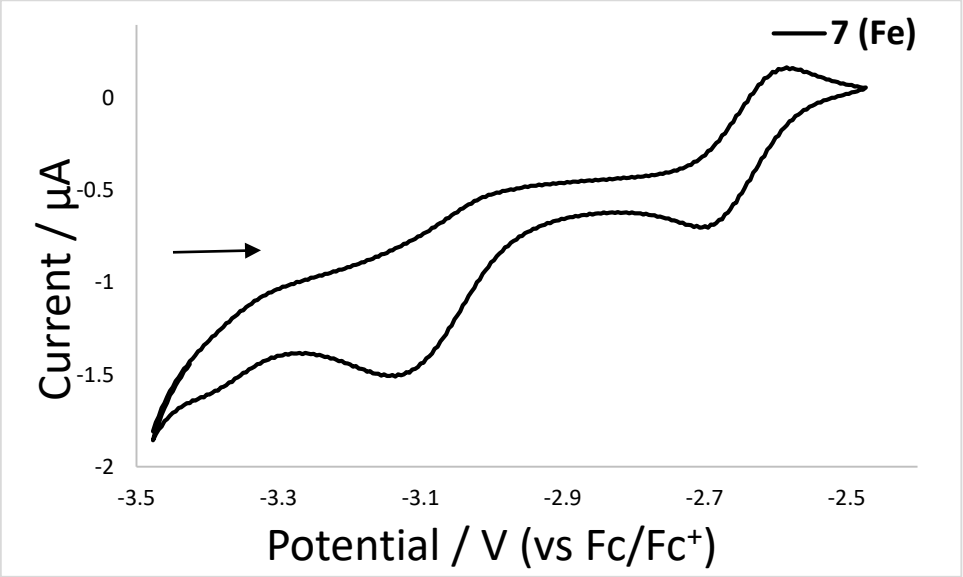

Figure S49. Cyclic voltammogram for complex **7** in THF (1 mM, 500 mV/s, 0.1 M [NBu_4][PF_6]).

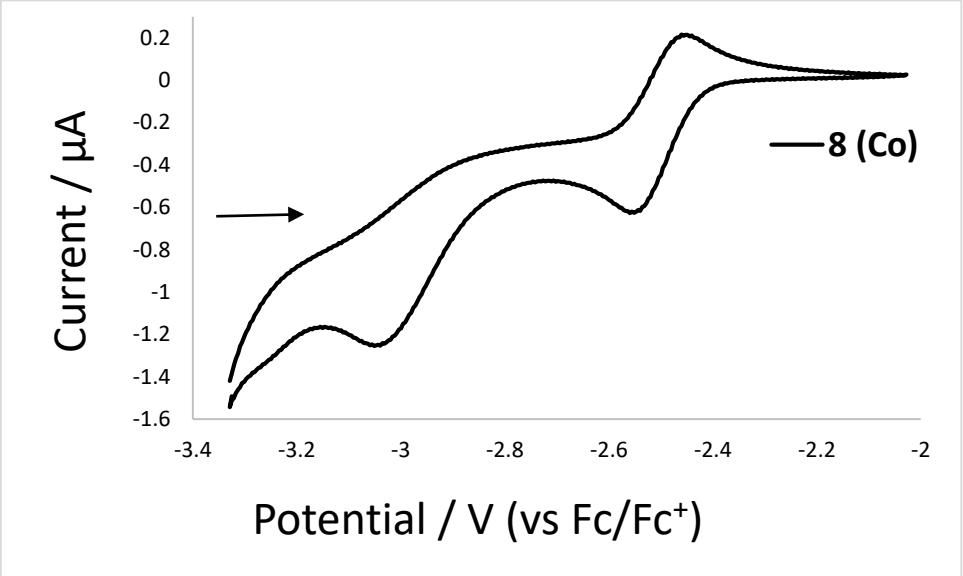

Figure S50. Cyclic voltammogram for complex **8** in THF (1 mM, 500 mV/s, 0.1 M [NBu_4][PF_6]).

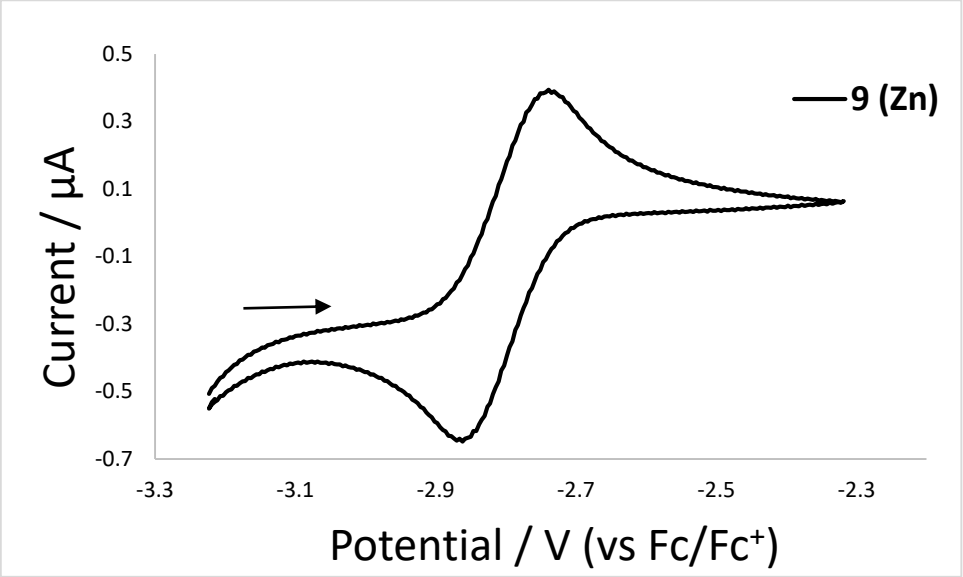

Figure S51. Cyclic voltammogram for complex **9** in THF (1 mM, 500 mV/s, 0.1 M [NBu_4][PF_6]).

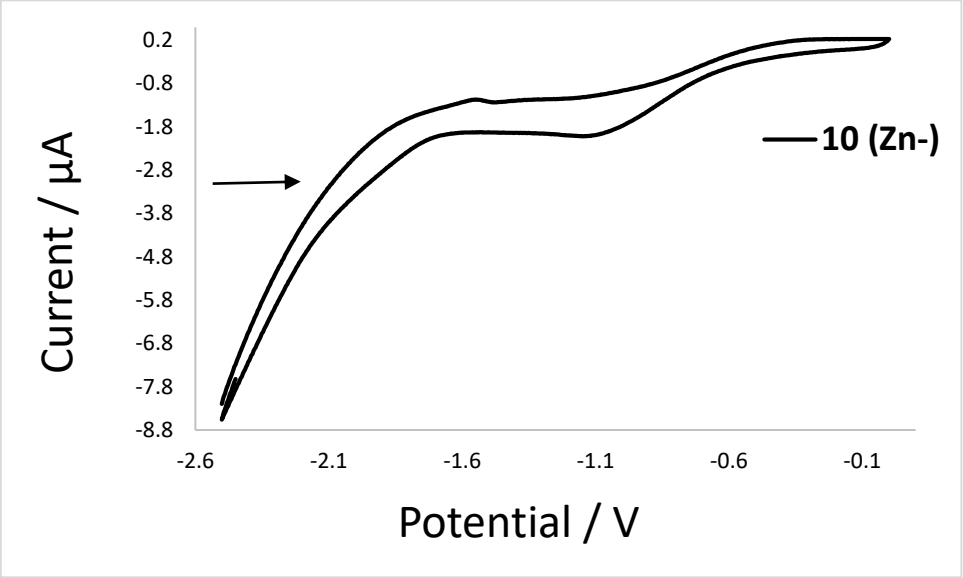

Figure S52. Cyclic voltammogram for complex **10** in THF (1 mM, 500 mV/s, 0.1 M [NBu_4][PF_6]).

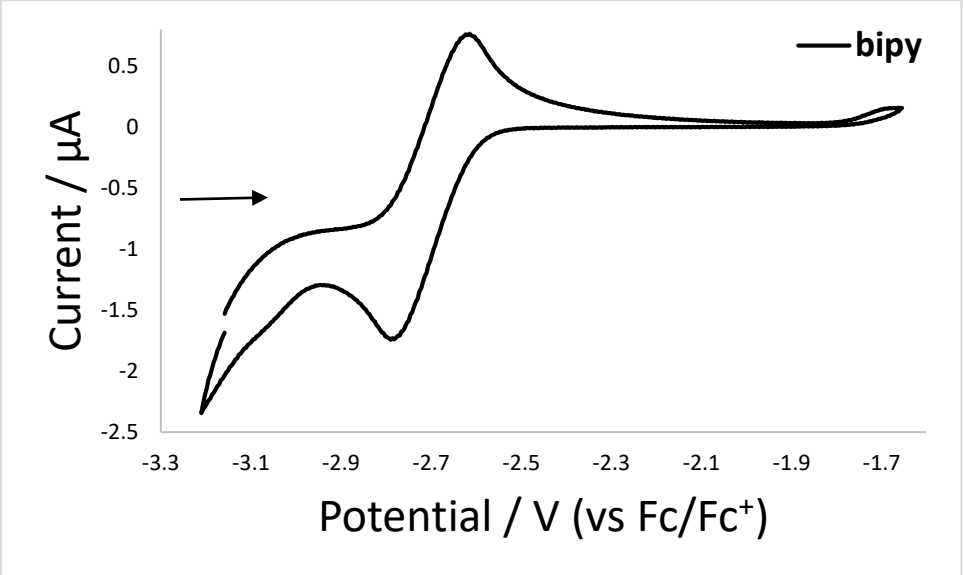

Figure S53. Cyclic voltammogram for 2,2′-bipyridine in THF (1 mM, 500 mV/s, 0.1 M [NBu_4][PF_6]).

6. X-Ray Diffraction Analysis and Molecular Structures

Data for **3** (CCDC 1918204), **4** (CCDC 1918205), **10** (CCDC 1918207) were collected at 100 K on a Bruker Quest D8 diffractometer using a graphite-monochromated Mo-Kα radiation and equipped with an Oxford Instrument Cooler Device. Data for **8** (CCDC 1918202), **1** (CCDC 1918208), **9** (CCDC 1918206) was collected at 100 K a STOE IPDS2 diffractometer and data for **2** (CCDC 1918203) were collected at 100 K a STOE IPDS2T diffractometer using a graphite-monochromated Mo-Kα radiation (λ = 0.71073 Å) and equipped with an Oxford Cryosystems Cryostream Cooler Device. The structures have been solved using either OLEX SHELXT V2014/1 [1] and refined by means of least-squares procedures on a F^2 with the aid of the program SHELXL-2016/6 [2] included in the software package WinGX version 1.63 [3] or using CRYSTALS [4].

The Atomic Scattering Factors were taken from International Tables for X-Ray Crystallography [5]. All non-hydrogen atoms were refined anisotropically. All hydrogens atoms were refined by using a riding model. Absorption corrections were introduced by using the MULTISCAN and X-Red program [6,7]. Drawings of molecules are performed with the program DIAMOND with 50% probability displacement ellipsoids for non-H atoms. Depiction of H atoms is omitted for clarity.

Table S1. Crystal data and structure refinement for **1**.

Identification Code	**K(18c6)Cr5**
Empirical formula	$C_{42}H_{84}CrKN_4O_8Si_4$
Formula weight	976.59
Temperature/K	100.0
Crystal system	triclinic
Space group	P−1
a/Å	11.6269(2)
b/Å	21.5546(4)
c/Å	21.8560(4)
α/°	95.633(2)
β/°	89.8920(10)
γ/°	90.377(2)
Volume/Å^3	5450.83(17)
Z	4
ρ_{calc} g/cm^3	1.190
μ/mm^{-1}	0.422
F(000)	2108.0
Crystal size/mm^3	0.3494 × 0.2903 × 0.2027
Radiation	Mo-Kα (λ = 0.71073)
2Θ range for data collection/°	3.504 to 50
Index ranges	−13 ≤ h ≤ 13, −25 ≤ k ≤ 25, −25 ≤ l ≤ 25
Reflections collected	88325
Independent reflections	19148 [R_{int} = 0.0630, R_{sigma} = 0.0368]
Data/restraints/parameters	19148/0/1112
Goodness-of-fit on F^2	1.073
Final *R* indexes [I>=2σ (I)]	R_1 = 0.0512, wR_2 = 0.1293
Final *R* indexes [all data]	R_1 = 0.0571, wR_2 = 0.1323
Largest diff. peak/hole/e Å^{-3}	0.79/−0.47

Table S2. Crystal data and structure refinement for **2**. The structure was refined as an inversion twin, twin ratio refined to 0.085(13).

Identification Code	**K(18c6)Mn6**
Empirical formula	$C_{34}H_{68}KMnN_4O_6Si_4$
Formula weight	835.32
Temperature/K	100.0
Crystal system	monoclinic
Space group	C2
a/Å	34.8403(17)
b/Å	18.4715(11)
c/Å	14.5302(8)
α/°	90
β/°	96.555(4)
γ/°	90
Volume/Å^3	9289.8(9)
Z	8
ρ_{calc} g/cm^3	1.194
μ/mm^{-1}	0.518
F(000)	3584.0
Crystal size/mm^3	0.27 × 0.18 × 0.07
Radiation	Mo-Kα (λ = 0.71073)
2Θ range for data collection/°	3.668 to 54.998
Index ranges	−45 ≤ h ≤ 43, −24 ≤ k ≤ 24, −18 ≤ l ≤ 18
Reflections collected	52126
Independent reflections	21354 [R_{int} = 0.0285, R_{sigma} = 0.0488]
Data/restraints/parameters	21354/1546/1264
Goodness-of-fit on F^2	0.917
Final *R* indexes [I>=2σ (I)]	R_1 = 0.0376, wR_2 = 0.0780
Final *R* indexes [all data]	R_1 = 0.0521, wR_2 = 0.0815
Largest diff. peak/hole / e Å^{-3}	0.81/−0.39

Table 3. Crystal data and structure refinement for **3**.

Identification Code	**K(18c6)Fe7**
Empirical formula	$C_{42}H_{83}FeKN_4O_8Si_4$
Formula weight	978.61
Temperature/K	100.0
Crystal system	triclinic
Space group	P−1
a/Å	10.8613(5)
b/Å	13.2627(6)
c/Å	19.8669(9)
α/°	77.5970(10)
β/°	80.062(2)
γ/°	83.452(2)
Volume/Å^3	2744.3(2)
Z	2
ρ_{calc} g/cm^3	1.184
μ/mm^{-1}	0.485
F(000)	1055.0
Crystal size/mm^3	0.21 × 0.2 × 0.11
Radiation	Mo-Kα (λ = 0.71073)
2Θ range for data collection/°	4.646 to 55.124
Index ranges	−14 ≤ h ≤ 14, −17 ≤ k ≤ 17, −25 ≤ l ≤ 25
Reflections collected	103782
Independent reflections	12642 [R_{int} = 0.0332, R_{sigma} = 0.0201]
Data/restraints/parameters	12642/276/683
Goodness-of-fit on F^2	1.054
Final *R* indexes [*I*>=2σ (*I*)]	R_1 = 0.0279, wR_2 = 0.0618
Final *R* indexes [all data]	R_1 = 0.0383, wR_2 = 0.0658
Largest diff. peak/hole/e Å^{-3}	0.34/−0.24

Table S4. Crystal data and structure refinement for **4**.

Identification Code	**K(18c6)Co8**
Empirical formula	$C_{42}H_{84}CoKN_4O_8Si_4$
Formula weight	983.52
Temperature/K	100.0
Crystal system	triclinic
Space group	P−1
a/Å	10.8097(5)
b/Å	13.2648(6)
c/Å	19.9051(10)
α/°	77.712(2)
β/°	80.199(2)
γ/°	83.606(2)
Volume/Å^3	2739.7(2)
Z	2
ρ_{calc} g/cm^3	1.192
μ/mm^{-1}	0.524
F(000)	1060.0
Crystal size / mm^3	0.23 × 0.14 × 0.07
Radiation	Mo-Kα (λ = 0.71073)
2Θ range for data collection/°	4.238 to 55.058
Index ranges	−14 ≤ h ≤ 14, −16 ≤ k ≤ 17, −25 ≤ l ≤ 25
Reflections collected	89930
Independent reflections	12549 [R_{int} = 0.0853, R_{sigma} = 0.0565]
Data/restraints/parameters	12549/57/584
Goodness-of-fit on F^2	1.017
Final *R* indexes [*I*>=2σ (*I*)]	R_1 = 0.0420, wR_2 = 0.0739
Final *R* indexes [all data]	R_1 = 0.0780, wR_2 = 0.0831
Largest diff. peak/hole/e Å^{-3}	0.29/−0.49

Table S5. Crystal data and structure refinement for **8**. The structure was refined as an inversion twin, twin ratio refined to 0.495(10).

Identification Code	**Co4**
Empirical formula	$C_{44}H_{88}Co_2N_8Si_8$
Formula weight	1071.80
Temperature/K	100
Crystal system	orthorhombic
Space group	P*ca*2$_1$
a/Å	18.7674(9)
b/Å	18.1030(8)
c/Å	17.5930(7)
α/°	90
β/°	90
γ/°	90
Volume/Å^3	5977.2(5)
Z	4
ρ_{calc} g/cm^3	1.191
μ/mm^{-1}	0.751
F(000)	2296.0
Crystal size/mm^3	0.31 × 0.2 × 0.2
Radiation	Mo Kα (λ = 0.71073)
2Θ range for data collection/°	3.89 to 51.998
Index ranges	−23 ≤ h ≤ 21, −19 ≤ k ≤ 22, −19 ≤ l ≤ 21
Reflections collected	20518
Independent reflections	10939 [R_{int} = 0.0219, R_{sigma} = 0.0228]
Data/restraints/parameters	10939/1/588
Goodness-of-fit on F^2	1.014
Final *R* indexes [*I*>=2σ (*I*)]	R_1 = 0.0280, wR_2 = 0.0670
Final *R* indexes [all data]	R_1 = 0.0307, wR_2 = 0.0679
Largest diff. peak/hole/e Å^{-3}	0.45/−0.25

Table S6. Crystal data and structure refinement for **9**. The structure was refined as an inversion twin, twin ratio refined to 0.292(9).

Identification Code	**Zn9**
Empirical formula	$C_{44}H_{88}N_8Si_8Zn_2$
Formula weight	1084.68
Temperature/K	100
Crystal system	orthorhombic
Space group	P*ca*2$_1$
a/Å	18.8806(12)
b/Å	18.0560(13)
c/Å	17.6133(17)
α/°	90
β/°	90
γ/°	90
Volume / Å^3	6004.5(8)
Z	4
ρ_{calc} g/cm^3	1.200
μ/mm^{-1}	0.994
F(000)	2320.0
Crystal size/mm^3	0.254 × 0.189 × 0.085
Radiation	Mo-Kα (λ = 0.71073)
2Θ range for data collection/°	4.314 to 51.996
Index ranges	−23 ≤ h ≤ 23, −21 ≤ k ≤ 22, −21 ≤ l ≤ 21
Reflections collected	52603
Independent reflections	11789 [R_{int} = 0.0737, R_{sigma} = 0.0589]
Data/restraints/parameters	11789/1/584
Goodness-of-fit on F^2	0.969
Final *R* indexes [*I*>=2σ (*I*)]	R_1 = 0.0340, wR_2 = 0.0700
Final *R* indexes [all data]	R_1 = 0.0445, wR_2 = 0.0718
Largest diff. peak/hole/e Å^{-3}	0.58/−0.21

Table S7. Crystal data and structure refinement for **10**.

Identification Code	**K(18c6)Zn10**
Empirical formula	$C_{38}H_{78}KN_4O_7Si_4Zn$
Formula weight	919.87
Temperature/K	100.0
Crystal system	monoclinic
Space group	$P2_1/c$
a/Å	12.1899(7)
b/Å	18.4365(10)
c/Å	22.8273(13)
α/°	90
β/°	95.423(2)
γ/°	90
Volume/Å^3	5107.2(5)
Z	4
ρ_{calc} g/cm^3	1.196
μ/mm^{-1}	0.700
F(000)	1980.0
Crystal size / mm^3	0.492 × 0.383 × 0.15
Radiation	Mo Kα (λ = 0.71073)
2Θ range for data collection/°	4.268 to 49.998
Index ranges	−14 ≤ h ≤ 14, −21 ≤ k ≤ 21, −27 ≤ l ≤ 27
Reflections collected	96672
Independent reflections	8987 [R_{int} = 0.0946, R_{sigma} = 0.0427]
Data/restraints/parameters	8987/1293/603
Goodness-of-fit on F^2	1.077
Final R indexes [I>=2σ (I)]	R_1 = 0.1301, wR_2 = 0.2536
Final R indexes [all data]	R_1 = 0.1530, wR_2 = 0.2636
Largest diff. peak/hole/e Å^{-3}	1.75/−1.94

Table S 8. Crystal data and structure refinement for **1**-**4**, **10**.

Identification code	K(18c6)Cr5	K(18c6)Mn6	K(18c6)Fe7	K(18c6)Co8	K(18c6)Zn10
Empirical formula	$C_{42}H_{84}CrKN_4O_8Si_4$	$C_{34}H_{68}KMnN_4O_6Si_4$	$C_{42}H_{83}FeKN_4O_8Si_4$	$C_{42}H_{84}CoKN_4O_8Si_4$	$C_{38}H_{78}KN_4O_7Si_4Zn$
Formula weight	976.59	835.32	978.61	983.52	919.87
Temperature / *K*	100.0	100.0	100.0	100.0	100.0
Crystal system	triclinic	monoclinic	triclinic	triclinic	monoclinic
Space group	P−1	C2	P−1	P−1	$P2_1/c$
a/Å	11.6269(2)	34.8403(17)	10.8613(5)	10.8097(5)	12.1899(7)
b/Å	21.5546(4)	18.4715(11)	13.2627(6)	13.2648(6)	18.4365(10)
c/Å	21.8560(4)	14.5302(8)	19.8669(9)	19.9051(10)	22.8273(13)
α/°	95.633(2)	90	77.5970(10)	77.712(2)	90
β/°	89.8920(10)	96.555(4)	80.062(2)	80.199(2)	95.423(2)
γ/°	90.377(2)	90	83.452(2)	83.606(2)	90
Volume/Å^3	5450.83(17)	9289.8(9)	2744.3(2)	2739.7(2)	5107.2(5)
Z	4	8	2	2	4
ρ_{calc} g/cm^3	1.190	1.194	1.184	1.192	1.196
μ/mm^{-1}	0.422	0.518	0.485	0.524	0.700
F(000)	2108.0	3584.0	1055.0	1060.0	1980.0
Crystal size/mm^3	0.3494 × 0.2903 × 0.2027	0.27 × 0.18 × 0.07	0.21 × 0.2 × 0.11	0.23 × 0.14 × 0.07	0.492 × 0.383 × 0.15
Radiation	Mo Kα (λ = 0.71073)	Mo Kα (λ = 0.71073)	Mo Kα (λ = 0.71073)	Mo Kα (λ = 0.71073)	Mo Kα (λ = 0.71073)
2Θ range for data collection/°	3.504 to 50	3.668 to 54.998	4.646 to 55.124	4.238 to 55.058	4.268 to 49.998
Index ranges	−13 ≤ h ≤ 13, −25 ≤ k ≤ 25, −25 ≤ l ≤ 25	−45 ≤ h ≤ 43, −24 ≤ k ≤ 24, −18 ≤ l ≤ 18	−14 ≤ h ≤ 14, −17 ≤ k ≤ 17, −25 ≤ l ≤ 25	−14 ≤ h ≤ 14, −16 ≤ k ≤ 17, −25 ≤ l ≤ 25	−14 ≤ h ≤ 14, −21 ≤ k ≤ 21, −27 ≤ l ≤ 27
Reflections collected	88325	52126	103782	89930	96672
Independent reflections	19148 [R_{int} = 0.0630, R_{sigma} = 0.0368]	21354 [R_{int} = 0.0285, R_{sigma} = 0.0488]	12642 [R_{int} = 0.0332, R_{sigma} = 0.0201]	12549 [R_{int} = 0.0853, R_{sigma} = 0.0565]	8987 [R_{int} = 0.0946, R_{sigma} = 0.0427]
Data/restraints/parameters	19148/0/1112	21354/1546/1264	12642/276/683	12549/57/584	8987/1293/603
Goodness-of-fit on F^2	1.073	0.917	1.054	1.017	1.077
Final *R* indexes [*I*>=2σ (*I*)]	R_1 = 0.0512, wR_2 = 0.1293	R_1 = 0.0376, wR_2 = 0.0780	R_1 = 0.0279, wR_2 = 0.0618	R_1 = 0.0420, wR_2 = 0.0739	R_1 = 0.1301, wR_2 = 0.2536
Final *R* indexes [all data]	R_1 = 0.0571, wR_2 = 0.1323	R_1 = 0.0521, wR_2 = 0.0815	R_1 = 0.0383, wR_2 = 0.0658	R_1 = 0.0780, wR_2 = 0.0831	R_1 = 0.1530, wR_2 = 0.2636
Largest diff. peak/hole/e Å^{-3}	0.79/−0.47	0.81/−0.39	0.34/−0.24	0.29/−0.49	1.75/−1.94

Table S9. Crystal data and structure refinement for **4** and **9**.

Identification Code	**Co4**	**Zn9**
Empirical formula	$C_{44}H_{88}Co_2N_8Si_8$	$C_{44}H_{88}N_8Si_8Zn_2$
Formula weight	1071.80	1084.68
Temperature / *K*	100	100
Crystal system	orthorhombic	orthorhombic
Space group	P*ca*2$_1$	P*ca*2$_1$
a/Å	18.7674(9)	18.8806(12)
b/Å	18.1030(8)	18.0560(13)
c/Å	17.5930(7)	17.6133(17)
α/°	90	90
β/°	90	90
γ/°	90	90
Volume / Å^3	5977.2(5)	6004.5(8)
Z	4	4
ρ_{calc} g/cm^3	1.191	1.200
μ/mm^{-1}	0.751	0.994
F(000)	2296.0	2320.0
Crystal size / mm^3	0.31 × 0.2 × 0.2	0.254 × 0.189 × 0.085
Radiation	Mo Kα (λ = 0.71073)	Mo Kα (λ = 0.71073)
2Θ range for data collection/°	3.89 to 51.998	4.314 to 51.996
Index ranges	−23 ≤ h ≤ 21, −19 ≤ k ≤ 22, −19 ≤ l ≤ 21	−23 ≤ h ≤ 23, −21 ≤ k ≤ 22, −21 ≤ l ≤ 21
Reflections collected	20518	52603
Independent reflections	10939 [R_{int} = 0.0219, R_{sigma} = 0.0228]	11789 [R_{int} = 0.0737, R_{sigma} = 0.0589]
Data/restraints/parameters	10939/1/588	11789/1/584
Goodness-of-fit on F^2	1.014	0.969
Final *R* indexes [*I*>=2σ (*I*)]	R_1 = 0.0280, wR_2 = 0.0670	R_1 = 0.0340, wR_2 = 0.0700
Final *R* indexes [all data]	R_1 = 0.0307, wR_2 = 0.0679	R_1 = 0.0445, wR_2 = 0.0718
Largest diff. peak/hole/e Å^{-3}	0.45/−0.25	0.58/−0.21

References

1. O. V. Dolomanov, L. J. Bourhis, R. J. Gildea, J. A. K. Howard, H. Puschmann, OLEX2: A Complete Structure Solution, Re-finement and Analysis Program. *J. Appl. Crytallogr*. **2009**, *42*, 339–441.
2. G. M. Sheldrick, *Acta Cryst*. **2015**, *71*, 3–8.
3. L.Farrugia, J. Appl. *Crystallogr*., **1999**, *32*, 837–838.
4. P. W. Betteridge, J. R. Carruthers, R. I. Cooper, K. Prout, D. J. Watkin *J. Appl. Cryst*. **2003**, *36*, 1487.
5. International Tables for X-ray crystallography (Kynoch Press, Birmingham, England, **1974**) *Vol*. *IV*.
6. Bruker AXS Inc. SADABS, 2016/2; Bruker AXS Inc.: Madison, WI, USA, 2016.
7. Stoe & Cie. X-Area, X-Red 1.63.1.0, 2002; Stoe & Cie: Darmstadt, Germany, 2016.